



Rose, H., Caminade, C., Bolajoko, M. B., Phelan, P., van Dijk, J., Baylis, M., Williams, D., & Morgan, E. R. (2016). Climate-driven changes to the spatio-temporal distribution of the parasitic nematode, *Haemonchus contortus*, in sheep in Europe. *Global Change Biology*, 22(3), 1271-1285. <https://doi.org/10.1111/gcb.13132>

Peer reviewed version

Link to published version (if available):  
[10.1111/gcb.13132](https://doi.org/10.1111/gcb.13132)

[Link to publication record in Explore Bristol Research](#)  
PDF-document

This is the author accepted manuscript (AAM). The final published version (version of record) is available online via Wiley at <http://onlinelibrary.wiley.com/doi/10.1111/gcb.13132/abstract>.

## University of Bristol - Explore Bristol Research

### General rights

This document is made available in accordance with publisher policies. Please cite only the published version using the reference above. Full terms of use are available:  
<http://www.bristol.ac.uk/red/research-policy/pure/user-guides/ebr-terms/>

**Climate-driven changes to the spatio-temporal distribution of the parasitic nematode, *Haemonchus contortus*, in sheep in Europe.**

**Running head: Climate change and *Haemonchus contortus* in Europe**

Hannah Rose<sup>1,2,3</sup>, Cyril Caminade<sup>4,5</sup>, Muhammad Bashir Bolajoko<sup>1,6</sup>, Paul Phelan<sup>7</sup>, Jan van Dijk<sup>8</sup>, Matthew Baylis<sup>4,9</sup>, Diana Williams<sup>10</sup>, Eric R. Morgan<sup>2,3</sup>

<sup>1</sup> School of Biological Sciences, Life Sciences Building, University of Bristol, Tyndall Avenue, Bristol, UK, BS8 1TQ

<sup>2</sup> School of Veterinary Sciences, University of Bristol, Langford House, Langford, Bristol, UK, BS40 5DU

<sup>3</sup> Cabot Institute, University of Bristol, Cantocks Close, Bristol, UK, BS8 1TS

<sup>4</sup> School of Environmental Sciences, University of Liverpool, UK

<sup>5</sup> Department of Epidemiology and Population Health, Institute of Infection and Global Health, University of Liverpool, The Farr Institute@HeRC, Liverpool, UK, L69 3GL

<sup>6</sup> National Veterinary Research Institute, P.M.B. 01, Vom, Plateau State, Nigeria

<sup>7</sup> Animal & Grassland Research and Innovation Centre, Teagasc, Grange, Dunsanny, Co. Meath, Ireland

<sup>8</sup> Department of Epidemiology and Population Health, Institute of Infection and Global Health, University of Liverpool, Leahurst, Neston, Cheshire, UK, CH64 7TE

<sup>9</sup> Health Protection Research Unit in Emerging and Zoonotic Infections, University of Liverpool, Neston, United Kingdom

<sup>10</sup> Department of Infection Biology, Institute of Infection and Global Health, University of Liverpool, Liverpool, UK, L3 5RF

**Corresponding author:** Email: hannah.rose@bristol.ac.uk Tel: +44 117 394 1383

**Keywords:** *Haemonchus contortus*, Q<sub>0</sub>, gastrointestinal nematode, climate change, Europe, adaptation, distribution shift, infection pressure, climate impact mitigation

**Type of paper:** original research article (primary research)

## Abstract

Recent climate change has resulted in changes to the phenology and distribution of invertebrates worldwide. Where invertebrates are associated with disease, climate variability and changes in climate may also affect the spatio-temporal dynamics of disease. Due to its significant impact on sheep production and welfare, the recent increase in diagnoses of ovine haemonchosis caused by the nematode *Haemonchus contortus* in some temperate regions is particularly concerning. This study is the first to evaluate the impact of climate change on *H. contortus* at a continental scale. A model of the basic reproductive quotient of macroparasites,  $Q_0$ , adapted to *H. contortus* and extended to incorporate environmental stochasticity and parasite behaviour, was used to simulate Pan-European spatio-temporal changes in *H. contortus* infection pressure under scenarios of climate change. Baseline  $Q_0$  simulations, using historic climate observations, reflected the current distribution of *H. contortus* in Europe. In northern Europe, the distribution of *H. contortus* is currently limited by temperatures falling below the development threshold during the winter months and within-host arrested development is necessary for population persistence over winter. In southern Europe *H. contortus* infection pressure is limited during the summer months by increased temperature and decreased moisture. Compared with this baseline,  $Q_0$  simulations driven by a climate model ensemble predicted an increase in *H. contortus* infection pressure by the 2080s. In northern Europe, a temporal range expansion was predicted as the mean period of transmission increased by 2-3 months. A bimodal seasonal pattern of infection pressure, similar to that currently observed in southern Europe, emerges in northern Europe due to increasing summer temperatures and decreasing moisture. The predicted patterns of change could alter the epidemiology of *H. contortus* in Europe, affect the future sustainability of contemporary

control strategies, and potentially drive local adaptation to climate change in parasite populations.

## Introduction

Recent climate change has been associated with observable changes in the phenology and geographic distribution of invertebrates worldwide (Parmesan & Yohe, 2003; Root et al., 2003; Altizer et al., 2013; Kutz et al., 2013). Where invertebrates are associated with disease, climate variability and changes in climate may also affect the spatio-temporal dynamics of disease (Lafferty, 2009; Guis et al., 2011; Rose & Wall, 2011; Wall & Ellse, 2011; Altizer et al., 2013; Kreppel et al., 2014). Trichostrongyloid gastrointestinal nematodes (GINs) are particularly vulnerable to such changes as part of the life-cycle is completed outside the host (Anderson, 2000) and development, mortality and behaviour of the free-living stages is climate-dependent (O'Connor et al., 2006; Sutherland & Scott, 2010; Hernandez et al., 2013). The impact of predicted climate change on the distribution of *Haemonchus contortus*, a highly pathogenic, blood-feeding GIN infecting sheep and goats, is of particular concern due to the severity of haemonchosis, a form of parasitic gastroenteritis caused by *H. contortus* infection, which results in significant morbidity and mortality associated with blood loss.

*Haemonchus contortus* is typically associated with tropical and sub-tropical climates (O'Connor et al., 2006) and climatic limitations play a dominant role in characterising its spatial distribution (O'Connor et al., 2006; Bolajoko et al., 2015; Rinaldi et al., 2015). The impact of climate change on the spatio-temporal distribution of *H. contortus* is of particular interest in Europe, where heterogeneity in its spatial distribution has been attributed to regional variation in mean temperature and rainfall (Rinaldi et al., 2015). For example, temperatures fall below the minimum development threshold of  $\sim 9^{\circ}\text{C}$  for at least part of the year in some northern (e.g. Sweden and the UK; Troell et al., 2005, Rose et al., 2015b) and alpine regions. In these regions, arrested development within the host is important for the survival over winter of populations of *H. contortus* (Waller et al., 2004), and limited

development and survival of the free-living stages during the cold season prevents infective stages accumulating on pasture, limiting infection pressure (Rose et al., 2015b).

Consequently, potential increases in winter air temperature of over 5°C in northern Europe (IPCC, 2013) could result in an increase in the development and survival of *H. contortus* on pasture during winter, with subsequent increases in infection pressure and disease incidence. Development of larvae is also limited during periods of drought (Eysker et al., 2005), which are more common in southern Europe. Effects of excessively high temperatures and low rainfall in summer might therefore act to offset improved winter conditions for transmission and alter the seasonal epidemiology of haemonchosis, with implications for optimal management interventions.

Climate change impacts are likely to be greatest where *H. contortus* exists at the edge of its range of climatic tolerance (Lafferty, 2009) and changes in the spatial distribution and prevalence of haemonchosis have already been observed in the United Kingdom in recent decades. Van Dijk et al. (2008) identified an increasing trend in diagnoses of haemonchosis between 1989 and 2006, associated with an increase in temperatures over the same period. Furthermore, the emergence of ovine haemonchosis in Scotland in recent years has been associated with climate warming (Kenyon et al., 2009). Further epidemiologically significant changes in the seasonality of infection pressure (Rose et al., 2015b) and spatial distribution of *H. contortus* are therefore expected under scenarios of future climate change.

The impact of any changes on welfare, productivity and profitability could be wide-ranging if farmers are unable to respond effectively to these changes. Increased agricultural inputs (e.g. pharmaceutical products and additional feed) and decreased welfare associated with climate-driven increases in prevalence of haemonchosis or range expansion of *H. contortus* present a real threat to the future sustainability of the European sheep industry. Furthermore, the threat

of anthelmintic resistance (Rose et al., 2015a) presents a significant constraint to the adaptive capacity of farmers to changes in disease dynamics in the face of global change. There is therefore a need to develop sustainable animal health management strategies which optimise the use of available resources, underpinned by a detailed understanding of the potential impacts of global changes, including climate and environmental management, on parasites and disease dynamics. Empirical evidence can be used to make qualitative predictions of parasite responses to climate change (e.g. Altizer et al., 2013). However, the present study is the first to quantify the impact of climate change on *H. contortus* at a continental scale. To evaluate potential future climate-driven changes in the risk of haemonchosis in Europe, and interactions with livestock management, a model based on the basic reproductive quotient of macroparasites,  $Q_0$  (Roberts & Heesterbeek, 1995), incorporating environmental stochasticity and sheep stocking density, was developed for *H. contortus* and applied at a Pan-European spatial scale.



## Materials and methods

### *Q<sub>0</sub> Model description*

The model was built on Roberts and Heesterbeek's (1995) basic reproduction quotient for macroparasites,  $Q_0$ , which provides a threshold quantity to predict the propensity of macroparasite populations to increase ( $Q_0 > 1$ ) or decrease ( $Q_0 < 1$ ) and therefore provides an index of infection pressure (Heesterbeek & Roberts, 1995; Roberts & Heesterbeek, 1995).  $Q_0$  estimates the average number of second-generation mature adult worms produced by a single adult worm during its lifetime in the absence of density-dependent constraints such as immunity and within-host competition, (Heesterbeek & Roberts, 1995).

Roberts and Heesterbeek (1995) applied the  $Q_0$  model (Equation 1) to the trichostrongylid nematode *Trichostrongylus colubriformis*, which, like *H. contortus*, follows a direct life cycle with in-host and free-living stages. Eggs are deposited on pasture in the faeces of the host where they hatch to produce larvae, which moult twice to reach the third, infective stage (L3). L3 then migrate horizontally out of the faeces when there is sufficient moisture and subsequently migrate between soil and herbage (vertical migration). L3 on herbage are accidentally ingested by the host during grazing, where upon they develop to the 4<sup>th</sup> larval stage (L4) and either undergo arrested development (hypobiosis) or continue to develop to the adult stage. Eggs produced by adult females are then passed in the sheep's (or goat's) faeces and the cycle continues. The  $Q_0$  model can be interpreted as sub-components, which characterise two key processes in the trichostrongylid life-cycle: the number of L3 produced by an adult worm during its lifetime (A), based on fecundity ( $\lambda$ ), adult mortality ( $\mu$ ) and the probability that an egg will develop to L3 ( $q$ ); the number of adult parasites produced by each L3 (B), based on the establishment rate of ingested L3 ( $p$ ), the mortality rate of L3 on pasture ( $\rho$ ), ingestion rate

of L3 by the host ( $\beta$ ) and the number of hosts ( $H$ ) (Roberts and Heesterbeek 1995). Parameters are defined in Table 1.

$$Q_0 = \underbrace{\frac{q\lambda}{\mu}}_A \underbrace{\frac{\beta p}{\rho + \beta H}}_B H \quad (1)$$

The parameter  $q$ , describing the probability of an egg developing to L3 was expanded (Equation 2) as described by Bolajoko et al. (2015) to incorporate climate-dependence in the life-history of free-living stages, and an additional horizontal migration parameter ( $m_1$ ). These changes allow for non-linear interactions between development ( $\delta$ ), survival ( $\mu_i$ ) and horizontal migration rates and address the importance of horizontal migration behaviour in determining the availability of L3 on pasture (Wang et al., 2014).

$$q = \frac{\delta m_1}{(\mu_e + \delta)(\mu_{l3} + m_1)} \quad (2)$$

A vertical migration parameter was added to the model in the present study,  $m_2$ , to reflect the distribution of infective third stage larvae (L3) between soil and herbage on pasture (Equation 3; Table 1).

$$Q_0 = \frac{q\lambda}{\mu} \frac{\beta p}{\rho + \beta H} H m_2 \quad (3)$$

The definition of  $Q_0$  in the present study is therefore extended to include environmental stochasticity. Thus,  $Q_0$  estimates, in the absence of density-dependent constraints and given current environmental conditions, the number of mature adult worms produced by a single

adult worm during its lifetime, and provides an instantaneous estimate of potential *H. contortus* infection pressure.

### ***Model parameterisation***

The proportion of total pasture L3 that are found on herbage,  $m_2$ , was set at a constant of 0.2 after van Dijk and Morgan (2011) recovered 20-30% of *H. contortus* L3 from herbage (corrected for recovery rate) and Callinan and Westcott (1986) recovered 4-23% of pasture L3 from herbage at temperatures between 10 and 30°C.

The functions for temperature-dependent development from egg to L3 ( $\delta$ ), and mortality of eggs ( $\mu_e$ ) and L3 ( $\mu_{l3}$ ) were derived from data in the literature as described previously (Rose et al., 2015b). Moisture rules constructed by Rose et al. (2015b) to estimate the effect of precipitation and evaporation on the development and migration of *H. contortus* were adapted to incorporate the combined effects of faecal moisture content on development and horizontal migration. Moisture availability in the 4 days preceding and following egg deposition is important for the development success and horizontal migration of *H. contortus* (O'Connor et al., 2008; Khadijah et al., 2013). Therefore a 9 day centred cumulative precipitation,  $P$ , and 9 day centred cumulative evaporation,  $E$ , was used to calculate  $P/E$  for each day. If  $P/E < 1$  then no eggs yielded L3 on pasture ( $q=0$ ), whereas if  $P/E \geq 1$  then the probability of development to L3 and migration onto pasture ( $q$ ) was estimated as a function of temperature (Table 1).

Temperature-dependent mortality rates of L3 on pasture,  $\rho$ , were estimated heuristically from the temperature-dependent mortality rates of L3 in faeces as described previously (Bolajoko et al., 2015).

Mean daily fecundity of adult female *H. contortus* was estimated to the nearest 100 from the results of individual experimental infections reported by Coyne and Smith (1992b). A 1:1 sex

ratio was assumed, therefore the mean fecundity per female worm was divided by 2 to estimate daily fecundity per adult worm,  $\lambda$ .

The instantaneous daily mortality rate of adult worms in the host,  $\mu$ , was estimated from the mean proportion of unlabelled adult worms surviving 8 weeks in sheep infected with between 0 and 6000 radiolabelled L3 per week (Table 1 in Barger & LeJambre, 1988) as  $-\ln(\text{mean proportion surviving})/56 \text{ days}$ . The mean proportion of unlabelled adults surviving 8 weeks was estimated by dividing the number of unlabelled adults recovered at necropsy on day 56 with the number of unlabelled adults recovered at necropsy on day 0.

The probability of establishment of *L3* following ingestion by the host,  $p$ , representative of immunologically naïve ovine hosts, was as reported by Barger et al. (Table 2 in Barger et al., 1985) for radiolabelled larvae administered to lambs that had been exposed to only 1 week of trickle infection with unlabelled larvae. Thus the labelled larvae that had established could be differentiated from the unlabelled larvae.

The rate at which larvae are ingested by host animals,  $\beta$ , was estimated as a function of herbage consumption rates,  $c$ , available biomass per unit area,  $B$ , and area of pasture,  $A$ , assuming that larvae are homogeneously distributed on pasture (Table 1).

### ***Current climate-driven variability in $Q_0$***

To describe the current climate-driven spatio-temporal variability in  $Q_0$  in Europe, the most up to date EOBS gridded climate dataset ( $0.25^\circ \times 0.25^\circ$ ) was used which is based on station measurements for Europe (Haylock et al., 2008). Rainfall ( $P$ ) and mean ( $T_{mean}$ ), minimum ( $T_{min}$ ) and maximum ( $T_{max}$ ) temperatures were available for the period 1950-2013 at daily temporal resolution. The model was applied to each cell in the gridded dataset and the resulting daily  $Q_0$  estimates were aggregated to estimate annual decadal averages and monthly decadal averages for the 1970s (1970-1979), 1980s (1980-1989), 1990s (1990-1999) and 2000s (2000-2009).

### ***Future climate-driven variability in $Q_0$***

To assess the impact of likely future climate change on the spatial variability of  $Q_0$  in Europe, a subset of five global climate models (HadGem2-ES; IPSL-CM5A-LR; MIROC-ESM-CHEM; GFDL-ESM2M; and NorESM1-M) produced within the Coupled Model Inter-Comparison Project 5 were used (Taylor et al., 2012). This subset was selected to give a wide range of predicted temperature and rainfall changes. As significant temperature and rainfall biases can be simulated by climate models with respect to climate observations, the simulated climatic variables were further calibrated by the Potsdam Institute for Climate Impact Research within the ISI-MIP project framework (Warszawski et al., 2014). This was carried out to ensure statistical agreement between the climate model outputs and the observed Watch Forcing Data dataset for 1960-1999 (Hempel et al., 2013). The  $Q_0$  model was applied to three time windows (20 year averages): 2020s (2011 to 2030); 2050s (2041-2060) and 2080s (2071-2090). All climate model experiments were re-gridded to a uniform half degree square grid at global scale and are presented as ensemble means (mean predictions from all five global climate models) for the European domain [ $35.5^\circ\text{N}$ - $71^\circ\text{N}$ ,  $12^\circ\text{W}$ - $30^\circ\text{E}$ ]. Data were available for four Representative Concentration Pathways (RCP) scenarios (RCP2.6, RCP4.5, RCP6.0, RCP8.5)

representing a range of radiative forcings, from the mildest (RCP2.6) to the most extreme (RCP8.5) emissions scenario (Moss et al., 2010).

Finally, to assess the overall impact of likely future climate change on seasonal variation in  $Q_0$  in Europe, mean monthly current and future  $Q_0$  estimates were calculated from the daily gridded estimates for the baseline period (1971-2010) using both EOBS data and the equivalent control (CTL) CMIP5 dataset, and for the 2080s under the RCP2.6 and RCP8.5 scenarios, for Northern Europe [48°N-59°N, 12°W-18.5°E] and Southern Europe [35.5°N-44°N, 10°W-18.5°E].

### ***Climate-management interactions***

The impact of climate-management interactions on  $Q_0$  predictions was explored by comparing estimates using the current climatic data and either a regionally variable sheep stocking density or a uniform host density of 1. All future  $Q_0$  estimates used the regionally variable sheep stocking density values. For this, a gridded dataset (0.25° x 0.25°) of livestock units (LSU) per hectare of pasture were derived from an aggregated NUTS 3 (Nomenclature Units for Territorial Statistics; EUROSTAT) regional sheep stocking density dataset (Fig. S1; Phelan et al., 2014). Data were presented in LSU per hectare and multiplied by 10 to obtain sheep per hectare (European Commission, 2009).

## Results

In the absence of moisture limitations,  $Q_0$  peaked at 20°C, decreasing at higher and lower temperatures due to a trade-off between development and mortality rates (Fig. 1).  $Q_0$  was zero below the predicted lower threshold for development of 9.16°C.

### *Current climate-driven variability in $Q_0$ and climate-management interactions*

There was considerable spatial variability in the annual mean decadal  $Q_0$  predictions (Fig. 2) associated with climate variability.  $Q_0 > 1$  (i.e. an increasing population) was predicted throughout Europe whereas  $Q_0 < 1$  (i.e. decreasing population) was restricted to a few scattered locations in Northern Italy, Eastern Poland, Norway, Bulgaria and the Austria-Slovakia border. Comparison of  $Q_0$  estimates using spatially variable and constant sheep stocking density ( $H=1$ ) (Fig. 3) indicates that  $Q_0$  is moderated by climate-management interactions whereby  $Q_0$  is increased by higher sheep stocking density (e.g. Norway) and decreased by low sheep stocking density (e.g. eastern Poland).

There was also significant seasonal variability in  $Q_0$  predictions across Europe. Throughout much of Europe,  $Q_0$  values below the critical threshold ( $Q_0=1$ ) were simulated during the winter months (December – February), indicating suppressed transmission and population decline (Figs. 4 & 5). In Norway, Sweden and Finland this period extended to October-May. Thus, between 1970 and 2013  $Q_0 < 1$  was predicted in these regions for 8 months of the year (Fig. 4).  $Q_0 > 1$  (an increasing population) was predicted for much of Europe between April and November as temperatures rose above the threshold for development (Figs. 4 & 5). However, in some Southern European regions such as Portugal and Spain, the opposite seasonal dynamic was predicted as temperatures remained sufficiently high over winter to allow the development

and survival of *H. contortus*, but conditions were unfavourable for *H. contortus* during the summer months due to increasing temperatures and decreased rainfall. As a result,  $Q_0 < 1$  (population decline) was predicted between June and August in some areas in southern Europe and mean  $Q_0$  for the region was low (Figs. 4 & 5b). Monthly decadal output using a variable and constant sheep stocking density is provided as supplementary information (Figs. S2-S9).

### ***Future climate-driven variability and patterns of change in predicted $Q_0$***

A general increase in future  $Q_0$  was predicted (Figs. 5 & 6), driving annual  $Q_0$  above the critical threshold throughout the majority of Europe under all RCPs and all time periods tested (Fig. 7). A greater change was predicted in northern Europe than in southern Europe (Figs. 5 & 6). There are large uncertainties in the multi-model projections. These uncertainties generally increase as a function of time and as a function of severity of emissions (Fig. 5).

The increase in mean annual  $Q_0$  estimates can be attributed to predicted increases year-round in northern Europe (Fig. 5a) and during the autumn and winter months in southern Europe (Fig. 5b). In addition, due to predicted increases in temperatures and moisture limitations during the summer months under the RCP8.5 scenario, a decrease in  $Q_0$  was simulated in northern Europe prior to the peak in September-October (Fig. 5a). This aligns more closely with the current bimodal seasonal pattern of  $Q_0$  in southern European regions, albeit with a significantly greater predicted  $Q_0$  than in current climate.



## Discussion

The impact of climate change on the spatio-temporal distribution of the haematophagous nematode, *H. contortus*, was investigated using an environmentally stochastic model of the basic reproductive quotient ( $Q_0$ ), which provides estimates of potential infection pressure given prevailing environmental conditions and a threshold quantity to estimate population persistence. Using baseline climatic data representative of the period 1971-2010,  $Q_0 < 1$  was predicted for northern Europe between November and March as low temperatures limit the development and survival of the free-living stages during the winter period. This reflects observations in these regions that *H. contortus* is dependent on the arrested development of fourth stage larvae in the host (hypobiosis; Waller et al., 2004; Sargison et al., 2007) and to a lesser extent L3 sequestered in soil (Rose et al., 2015b) to survive the winter period. Simulations using both the RCP2.6 and RCP8.5 climate change scenarios predicted a mean increase in the future transmission season of 2-3 months such that mean  $Q_0$  is greater than 1 throughout the year in northern Europe. This predicted future increase in infection pressure in northern Europe may result in an increased incidence of haemonchosis if current control strategies are insufficient and farmers fail to adapt. Furthermore, simulations of *H. contortus* population dynamics suggest that the extended period where temperatures remain above the threshold for development may magnify the predicted increase in infection pressure as a result of an increase in cumulative pasture contamination, and a decrease in total L3 mortality during periods that are unfavourable for development (Rose et al., 2015b). The predicted shift in the geographical range of the free-living stages of *H. contortus* during the winter months may relinquish *H. contortus* of the selection pressures driving winter hypobiosis (Gaba & Gourbière, 2008), presenting a target for local adaptation to climate change, and increasing infection pressure during this period.

In addition to the predicted increase in infection pressure during the winter months in northern Europe, a decrease in infection pressure during the late summer months was predicted due to an interaction between increased temperature-dependent mortality and development rates, and moisture limitations on development success and migration onto pasture ( $q$ ). This was more pronounced under RCP8.5 than RCP2.6. The emergence of a bimodal pattern of seasonal infection pressure appears to be a consistent prediction for GINs in temperate and Arctic regions under various scenarios of climate change; a similar pattern was predicted for the GINs *H. contortus*, *Teladorsagia circumcincta* and *Ostertagia ostertagi* infecting ruminants in England (Rose et al., 2015b), and *O. gruehneri* infecting caribou in North America (Molnár et al., 2013), as well as other parasitic helminths in northern Europe (*Fasciola hepatica*; Caminade et al., 2015) and invertebrate ectoparasites in Great Britain (*Lucilia sericata*; Rose & Wall, 2011; Wall & Ellse, 2011). This “summer dip” in infection pressure may play a role in moderating the impact of climate change in northern Europe (Rose et al., 2015b).

The predicted future bimodal pattern of infection pressure predicted for *H. contortus* in northern Europe is currently observed in southern Europe where, on average, winter temperatures are high enough to permit development and survival of the free-living stages, yet moisture limitations and high temperatures during the summer months limit development success.  $Q_0$  is predicted to increase in southern Europe during the winter months under RCP8.5, while a longer summer break in transmission is predicted where  $Q_0$  falls below 1. In contrast to the decrease in selection pressure for winter hypobiosis in northern Europe, hypobiosis may become increasingly important as a strategy for the future summer survival of *H. contortus* in southern Europe due to the predicted future reduction in  $Q_0$  during the hot, dry summer months increasing the selection pressure for summer hypobiosis. Similar patterns

are seen in semi-arid regions such as Kenya, where hypobiosis is an important strategy for the survival of *H. contortus* during the dry periods when the transmission of free-living stages is limited (Gatongi et al., 1998).

In addition to climate variability other environmental and livestock management factors that may affect disease risk vary from region to region within Europe due to differing socio-economic, policy and bioclimatic drivers e.g. land use and stocking rates. The contribution of livestock management to spatial variability in disease risk may even outweigh the contribution of climate and provide an opportunity to mitigate the impact of climate change (Morgan & Wall, 2009). By considering the interacting effects of host (sheep) stocking density and climate on  $Q_0$  insights have been gained into the drivers of spatial variability in disease risk. Sheep stocking density moderated the effect of climate variability, increasing spatial heterogeneity in  $Q_0$  predictions. For the majority of Europe, a higher  $Q_0$  was predicted under current regional sheep stocking densities compared with a constant sheep stocking density (1 sheep ha<sup>-1</sup>), suggesting that current European sheep stocking densities enhance infection pressure and transmission risk of *H. contortus*. Therefore, predicted future increases in infection will be exacerbated in regions where high future stocking densities are necessary due to limitations such as land availability. However, the extent to which environment and livestock management are likely to change in response to climate change and altered patterns of parasite transmission is difficult to estimate, particularly where host immunity, farm/environmental management, climate and parasites interact (Rohr et al., 2011), and where economic considerations are of paramount importance. Furthermore, the behaviour of farm managers may lag behind the optimal response to climate-driven changes, for example due to variability in adaptive capacity and perception of resilience and risk (Marshall, 2010). As a result, it is common, as in this study, to make climate change impact assessments under

the assumption of no change in management. Some recent progress has been made in estimating the impact of climate change on management factors relevant to the epidemiology of gastrointestinal helminths such as *H. contortus*, such as grazing season length (Phelan et al., 2015). However, this remains a knowledge gap that can largely only be addressed by evaluation of comparative management scenarios (Morgan & Wall, 2009; Wall & Ellse, 2011).

A previous adaptation of the  $Q_0$  model to *H. contortus* was successful in replicating broad-scale regional variation in frequency of *H. contortus* in the gastrointestinal nematode fauna of sheep (Bolajoko et al., 2015). Using daily climatic data and with the addition of a vertical migration parameter and variable sheep stocking density, the  $Q_0$  model presented here replicates qualitative spatio-temporal patterns of infection pressure, intensity of infection and incidence of haemonchosis in Europe. The predicted optimal conditions for  $Q_0$  were similar to those previously observed experimentally *in vitro* (Coyne & Smith, 1992a) and *in vivo* (Rose, 1963). In the UK, peak diagnoses of haemonchosis are generally made between July and October (van Dijk et al., 2008) corresponding with the peak  $Q_0$  predictions for the region. In Sweden, the absence of infection by *H. contortus* in naive lambs turned out onto pasture in May (tracer lambs) indicates minimal overwinter survival of *H. contortus* on pasture in the region (Waller et al., 2004) and reflects the extended period where  $Q_0 < 1$  was predicted for the majority of Sweden in the current study. The predicted decrease in summer  $Q_0$  in southern and Mediterranean regions is reflected in previously observed decreases in the recovery of *H. contortus* infective stages from pasture samples in North Limousin, France, during the summer months (Gruner et al., 1980) and reduced intensity of *H. contortus* infection during the summer in naturally infected goats in Central Spain compared with spring and autumn (Valcárcel & Romerro, 1999).

Potential limitations of the  $Q_0$  approach adopted here lie primarily in the instantaneous nature of the model. For example, the cumulative impact of changes in development and survival of free-living stages on seasonal and inter-annual variation in infection pressure are not captured by the  $Q_0$  model. Furthermore, the development of immunity and the annual rise in faecal egg counts in ewes around the time of parturition (periparturient rise) due to the relaxation of immunity and subsequent resumption of development of larvae that have overwintered as hypobiotic larvae in the host is not included in the model. Therefore changes in the magnitude of the periparturient rise as a result of changes in infection pressure in the previous grazing season are not predicted. However, additional complexity is required to incorporate host-parasite interactions in sufficient detail to capture these processes e.g. Learmount et al. (2006). The simplicity of the  $Q_0$  models thus provides a tractable solution to predicting patterns of change in infection pressure and disease risk in response to changing climate and management at broad spatial and temporal scales. This is especially appropriate for *H. contortus*, in which egg shedding rates are often high and transmission success depends largely on climatic conditions over a short period of time. General predictions of likely changes in seasonal patterns of transmission potential, such as presented here, are likely to usefully inform parasite control strategies even without additional biological and management detail e.g. by identifying regions where climate change is predicted to have the greatest impact (Rohr et al., 2011).

In conclusion, an overall increase in infection pressure is predicted for *H. contortus* in Europe under a range of climate change scenarios. Predicted increases and changes in seasonal patterns of infection pressure were greater in northern Europe than in southern Europe, supporting the hypothesis that climate change impacts will be greatest where species exist at the edge of their range (Lafferty, 2009; Rohr et al., 2011), and suggesting that sheep and goat

producers in northern Europe are likely to be hardest hit by climate change impacts on *H. contortus*. Failure to adapt management to these changes could significantly impact animal welfare and threaten the future sustainability of the livestock industry in affected regions.

## **Competing interests**

We have no competing interests

## **Authors' contributions**

HR extended the  $Q_0$  model and defined model parameters, participated in the design of the study and prepared the manuscript; CC acquired and prepared climatic data, carried out model integrations, participated in the design of the study and prepared the manuscript; MBB contributed to the development of the climate-dependent model components; PP acquired and prepared livestock stocking density data and participated in the design of the study; JvD designed and coordinated the study; MB and DW participated in the study design; ERM conceived, designed and coordinated the study. All authors contributed to early drafts of the manuscript and gave final approval for publication.

## **Acknowledgments**

We acknowledge the ISI-MIP Fast Track project, funded by the German Federal Ministry of Education and Research (BMBF) with project funding reference number 01LFIG. S1201A, for providing the climate model experiments.

We acknowledge the E-OBS dataset from the EU-FP6 project ENSEMBLES (<http://ensembles-eu.metoffice.com>) and the data providers in the ECA&D project (<http://www.ecad.eu>). We acknowledge the World Climate Research Programme's Working

228 Group on Coupled Modelling, which is responsible for CMIP, and we thank the Met Office  
229 Hadley Centre climate modeling groups for producing and making available their model  
230 output. For CMIP the U.S. Department of Energy's Program for Climate Model Diagnosis and  
231 Intercomparison provides coordinating support and led development of software infrastructure  
232 in partnership with the Global Organization for Earth System Science Portals.  
233 We also thank two anonymous reviewers for their comments.

#### 234 **Funding**

235 The authors acknowledge funding support from the GLOWORM EU-FP7 project (contract  
236 number FP7-KBBE-2011-5-288975). CC was also supported by The Farr Institute for Health  
237 Informatics Research (MRC grant: MR/M0501633/1)

## References

- Altizer S, Ostfeld RS, Johnson PTJ, Kutz S, Harvell CD (2013) Climate change and infectious diseases: from evidence to a predictive framework. *Science*, **341**, 514-519. (doi: 10.1126/science.1239401)
- Anderson RC (2000) *Nematode parasites of vertebrates: their development and transmission*. CAB International Publishing, Oxon, UK.
- Anon (2002) WATFLOOD Distributed Hydrologic Modelling: User manual. Available at: [http://www.civil.uwaterloo.ca/watflood/Manual/02\\_03\\_2.htm](http://www.civil.uwaterloo.ca/watflood/Manual/02_03_2.htm). Accessed 16/02/2015
- Barger IA, Le Jambre LF (1988) Regulation of *Haemonchus contortus* populations in sheep: Mortality of established worms. *International Journal for Parasitology*, **18**, 269–273. (doi:10.1016/0020-7519(88)90067-7)
- Barger IA, Le Jambre LF, Georgi JR, Davies HI (1985) Regulation of *Haemonchus contortus* populations in sheep exposed to continuous infection. *International Journal for Parasitology*, **15**, 529–533. (doi:10.1016/0020-7519(85)90049-9)
- Bolajoko MB, Rose H, Musella V, Bosco A, Rinaldi L, van Dijk J, Cringoli G, Morgan ER (2015) The basic reproduction quotient ( $Q_0$ ) as a spatial predictor of the seasonality of ovine haemonchosis. *Geospatial Health*, **9**, 333-350. (doi: 10.4081/gh.2015.356)
- Callinan APL, Westcott JM (1986) Vertical distribution of trichostrongylid larvae on herbage and in soil. *International Journal for Parasitology*, **16**, 241–244. (doi:10.1016/0020-7519(86)90050-0)



258 Caminade C, van Dijk J, Baylis M, Williams D (2015) Modelling recent and future climatic  
 259 suitability for fasciolosis in Europe. *Geospatial Health*, **9**, 301-308. (doi:  
 260 10.4081/gh.2015.352)

261 Coyne MJ, Smith G (1992a) The development and mortality of the free-living stages of  
 262 *Haemonchus contortus* in laboratory culture. *International Journal for Parasitology*, **22**, 641-  
 263 650. (doi:10.1016/0020-7519(92)90013-B)

264 Coyne MJ, Smith G (1992b) The mortality and fecundity of *Haemonchus contortus* in  
 265 parasite-naïve and parasite-exposed sheep following single experimental infections.  
 266 *International Journal for Parasitology*, **22**, 315–325. (doi:10.1016/S0020-7519(05)80009-8)

267 European Commission (2009) Commission regulation 1200/2009 of 30 November 2009  
 268 implementing regulation 1166/2008 of the European Parliament and of the Council on farm  
 269 structure surveys (FSS) and the survey on agricultural production methods (SAPM), as  
 270 regards livestock unit coefficients and definitions of the characteristics. *Official Journal of*  
 271 *the European Union*, **L329**, 23-28.

272 Eysker M, Bakker N, Kooyman E, van der Linden D, Schrama C, Ploeger HW. (2005)  
 273 Consequences of the unusually warm and dry summer of 2003 in The Netherlands: Poor  
 274 development of free living stages, normal survival of infective larvae and long survival of  
 275 adult gastrointestinal nematodes of sheep. *Veterinary Parasitology*, **133**, 313-  
 276 321. (doi:10.1016/j.vetpar.2005.05.058)

277 Gaba S, Gourbière S (2008) To delay once or twice: the effect of hypobiosis and free-living  
 278 stages on the stability of host-parasite interactions. *Journal of the Royal Society Interface*, **5**,  
 279 919-928. (doi:10.1098/rsif.2007.1282)

280 Gatongi PM, Prichard RK, Ranjan S, Gathuma JM, Munyua WK, Cheruiyot H, Scott ME  
 281 (1998) Hypobiosis of *Haemonchus contortus* in natural infections of sheep and goats in a  
 282 semi-arid area of Kenya. *Veterinary Parasitology*, **77**, 49-61. (doi:10.1016/S0304-  
 283 4017(97)00207-0)

284 Gruner L, Mauleon H, Huberts J, Sauve C (1980) A study of ovine gastro-intestinal  
 285 strongylosis in a sheep flock on permanent pasture II. Population dynamics of parasites on  
 286 the pasture in 1977 and an epidemiological interpretation. *Annales de Recherches*  
 287 *Vétérinaires*, **11**, 133-140.

288 Guis H, Caminade C, Calvete C, Morse AP, Tran A, Baylis M (2011) Modelling the effects  
 289 of past and future climate on the risk of bluetongue emergence in Europe. *Journal of the*  
 290 *Royal Society Interface*, **9**, 339-350. (doi: 10.1098/rsif.2011.0255)

291 Hargreaves GH and Samani ZA (1985) Reference crop evapotranspiration from temperature.  
 292 *Applied Engineering in Agriculture*, **1**(2), 96-99.

293 Haylock MR, Hofstra N, Klein Tank AMG, Klok EJ, Jones PD, New M (2008) A European  
 294 daily high-resolution gridded dataset of surface temperature and precipitation. *Journal of*  
 295 *Geophysical Research: Atmospheres*, **113**, D20119. (doi:10.1029/2008JD10201)

296 Heesterbeek JAP, Roberts MG (1995). Threshold quantities for helminth infections. *Journal*  
 297 *of Mathematical Biology*, **33**, 415-434.

298 Hempel S, Frieler K, Warszawski L, Schewe J, Piontek F (2013) A trend-preserving bias  
 299 correction – the ISI-MIP approach. *Earth System Dynamics*, **4**, 49-92. (doi:10.5194/esd-4-  
 300 219-2013)

301 Hernandez AD, Poole A, Cattadori IM (2013) Climate changes influence free-living stages of  
 302 soil-transmitted parasites of European rabbits. *Global Change Biology*, **19**, 1028-1042. (doi:  
 303 10.1111/gcb.12106)

304 IPCC (2013) *Annex I: Atlas of Global and Regional Climate Projections* (van Oldenborgh  
 305 GJ, Collins M, Arblaster J, Christensen JH, Marotzke J, Power SB, Rummukainen M, Zhou  
 306 T (eds.)). In: *Climate Change 2013: The Physical Science Basis. Contribution of Working*  
 307 *Group I to the Fifth Assessment Report of the Intergovernmental Panel on Climate Change*  
 308 (Stocker TF, Qin D, Plattner G-K, Tignor M, Allen SK, Boschung J, Nauels A, Xia Y, Bex  
 309 V, Midgley PM (eds.)). Cambridge University Press, Cambridge, UK.

310 Kao RR, Leathwick DM, Roberts MG, Sutherland IA (2000) Nematode parasites of sheep: a  
 311 survey of epidemiological parameters and their application in a simple model. *Parasitology*,  
 312 **121**, 85–103.

313 Kenyon F, Sargison ND, Skuce PJ, Jackson F (2009) Sheep helminth parasitic disease in  
 314 south-eastern Scotland arising as a possible consequence of climate change. *Veterinary*  
 315 *Parasitology*, **163**, 293-297. (doi:10.1016/j.vetpar.2009.03.027)

316 Khadijah S, Kahn LP, Walkden-Brown SW, Bailey JN, Bowers SF (2013) Effect of  
 317 simulated rainfall timing on faecal moisture and development of *Haemonchus contortus* and  
 318 *Trichostrongylus colubriformis* eggs to infective larvae. *Veterinary Parasitology*, **192**, 199–  
 319 210. (doi:10.1016/j.vetpar.2012.10.015)

320 Kreppel KS, Caminade C, Telfer S, Rajerison M, Rahalison L, Morse A, Baylis M (2014) A  
 321 non-stationary relationship between global climate phenomena and human plague incidence  
 322 in Madagascar. *PLOS Neglected Tropical Diseases*, **8**, e3155.  
 323 (doi:10.1371/journal.pntd.0003155)

324 Kutz SJ, Checkley S, Verocai GG, Mathieu D, Hoberg EP, Peacock R, Wu JP, Orsel K,  
 325 Seegers K, Warren AL, Abrams A (2013) Invasion, establishment, and range expansion of  
 326 two parasitic nematodes in the Canadian Arctic. *Global Change Biology*, **19**, 3254-3262.  
 327 (doi: 10.1111/gcb.12315)

328 Lafferty KD (2009) The ecology of climate change and infectious diseases. *Ecology*, **90**, 888-  
 329 900.

330 Learmount J, Taylor MA, Smith G, Morgan C (2006) A computer model to simulate control  
 331 of parasitic gastroenteritis in sheep on UK farms. *Veterinary Parasitology*, **412**, 312-329.  
 332 (doi:10.1016/j.vetpar.2006.07.012)

333 Marshall NA. 2010 Understanding social resilience to climate variability in primary  
 334 enterprises and industries. *Glob. Env. Change* **20**, 36-43.  
 335 (doi:10.1016/j.gloenvcha.2009.10.003)

336 Molnár PK, Kutz SJ, Hoar BM, Dobson AP (2013) Metabolic approaches to understanding  
 337 climate change impacts on seasonal host-macroparasite dynamics. *Ecology Letters*, **16**, 9-21.  
 338 (doi:10.1111/ele.12022)

339 Morgan ER, Wall R (2009) Climate change and parasitic disease: farmer mitigation?. *Trends*  
 340 *in Parasitology*, **25**, 308-313. (doi:10.1016/j.pt.2009.03.012)

341 Moss RH, Edmonds JA, Hibbard KA, Manning MR, Rose SK, van Vuuren DP, Carter TR,  
 342 Emori S, Kainuma M, Kram T, Meehl GA, Mitchell JFB, Nebojsa N, Riahi K, Smith SJ,  
 343 Stouffer RJ, Thomson AM, Weyant JP, Wilbanks TJ (2010) The next generations of  
 344 scenarios for climate change research and assessment. *Nature*, **463**, 747-756. (doi:  
 345 10.1038/nature08823)

346 O'Connor LJ, Kahn LP, Walkden-Brown SW (2008) Interaction between the effects of  
 347 evaporation rate and amount of simulated rainfall on development of the free-living stages of  
 348 *Haemonchus contortus*. *Veterinary Parasitology*, **155**, 223–34.  
 349 (doi:10.1016/j.vetpar.2008.05.010)

350 O'Connor LJ, Walkden-Brown SW, Kahn LP (2006) Ecology of the free-living stages of  
 351 major trichostrongylid parasites of sheep. *Veterinary Parasitology*, **142**, 1-15.

352 Parmesan C, Yohe G (2003) A globally coherent fingerprint of climate change impacts across  
 353 natural systems. *Nature*, **421**, 37-42. (doi:10.1038/nature01286)

354 Phelan P, Morgan ER, Rose H, O'Kiely P (2014) Multiple regression analysis of the  
 355 relationship between bioclimatic variables and grazing season length on European dairy, beef  
 356 and sheep farms. In: *The Future of European Grasslands; 25th General Meeting of the*  
 357 *European Grassland Federation* (Hopkins A, Collins RP, Fraser MD, King VR, Lloyd DC,  
 358 Moorby JM, Robson PRH (eds.)), 7-11 September, Aberystwyth, Wales. pp. 100-102.

359 Phelan P, Morgan ER, Rose H, Grant J, O'Kiely P (2015) Future grazing season length  
 360 predictions for European dairy, beef and sheep farms based on current regression with  
 361 bioclimatic variables. *Journal of Agricultural Science*, *in press*.  
 362 (doi:10.1017/S0021859615000830).

363 Rinaldi L, Catelan D, Musella V, Cecconi L, Hertzberg H, Torgerson PR, Mavrot F, de Waal  
 364 T, Selemetas N, Coll T, Bosco A, Biggeri A, Cringoli G (2015) *Haemonchus contortus*:  
 365 spatial risk distribution for infection in sheep in Europe. *Geospatial Health*, **9**, 325-331. (doi:  
 366 10.4081/gh.2015.355)

367 Roberts MG, Heesterbeek JAP (1995) The dynamics of nematode infections of farmed  
 368 ruminants. *Parasitology*, **110**, 493-502. (doi:10.1017/S0031182000064830)

369 Rohr JR, Dobson AP, Johnson PTJ, Kilpatrick AM, Paull SH, Raffel TR, Ruiz-Moreno D,  
 370 Thomas MB (2011) Frontiers in climate change-disease research. Trends in Ecology and  
 371 Evolution, **26**, 270-277. (doi:10.1016/j.tree.2011.03.002)

372 Root TL, Price JT, Hal KR, Schneider SH, Rosenzweig C, Pounds JA (2003) Fingerprints of  
 373 global warming on wild animals and plants. Nature, **421**, 57-60. (doi:10.1038/nature01333)

374 Rose JH (1963) Observations on the free-living stages of the stomach worm *Haemonchus*  
 375 *contortus*. Parasitology, **53**, 469-481. (doi:10.1017/S0031182000073923)

376 Rose H, Wall R (2011) Modelling the impact of climate change on spatial patterns of disease  
 377 risk: sheep blowfly strike by *Lucilia sericata* in Great Britain. International Journal for  
 378 Parasitology, **41**, 739-746. (doi:10.1016/j.ijpara.2011.01.012)

379 Rose H, Rinaldi L, Bosco A, Mavrot F, de Waal T, Skuce P, Charlier J, Torgerson PR,  
 380 Hertzberg H, Hendrickx G, Vercruysse J, Morgan ER (2015a). Widespread anthelmintic  
 381 resistance in European farmed ruminants: a systematic review. Veterinary Record, **176**, 546.  
 382 (doi:10.1136/vr.102982)

383 Rose H, Wang T, van Dijk J, Morgan ER (2015b) GLOWORM-FL: a simulation model of  
 384 the effects of climate and climate change on the free-living stages of gastro-intestinal  
 385 nematode parasites of ruminants. Ecological Modelling, **297**, 232-245.  
 386 (doi:10.1016/j.ecolmodel.2014.11.033)

387 Sargison ND, Wilson DJ, Bartley DJ, Penny CD, Jackson F (2007) Haemonchosis and  
 388 teladorsagiosis in a Scottish sheep flock putatively associated with the overwintering of  
 389 hypobiotic fourth stage larvae. Veterinary Parasitology, **147**, 326-331.  
 390 (doi:10.1016/j.vetpar.2007.04.011)

391 Sutherland I, Scott I (2010) *Gastrointestinal nematodes of sheep and cattle*. Wiley-Blackwell,  
392 Sussex, UK.

393 Taylor KE, Stouffer RJ, Meehl GA (2012) An overview of CMIP5 and the experiment  
394 design. Bulletin of the American Meteorological Society, **93**, 485–498. (doi:10.1175/BAMS-  
395 D-11-00094.1)

396 Troell K, Waller P, Höglund J (2005) The development and overwintering survival of free-  
397 living larvae of *Haemonchus contortus* in Sweden. Journal of Helminthology, **79**, 373-379.  
398 (doi:10.1079/JOH2005286)

399 Valcárcel F, Romerro CG (1999) Prevalence and seasonal pattern of caprine trichostrongyles  
400 in a dry area of Central Spain. Journal of Veterinary Medicine Series B, **46**, 673-681.  
401 (doi:10.1046/j.1439-0450.1999.00297.x)

402 van Dijk J, David GP, Baird G, Morgan ER (2008) Back to the future: developing hypotheses  
403 on the effects of climate change on ovine parasitic gastroenteritis from historical data.  
404 Veterinary Parasitology, **158**, 73-84. (doi:10.1016/j.vetpar.2008.08.006)

405 van Dijk J, Morgan ER (2011) The influence of water on the migration of infective  
406 trichostrongyloid larvae onto grass. Parasitology, **138**, 780–788.  
407 (doi:10.1017/S0031182011000308)

408 Wall R, Ellse L (2011) Climate change and livestock parasites: integrated management of  
409 sheep blowfly strike in a warmer environment. Global Change Biology, **17**, 1770-1777.  
410 (doi:10.1111/j.1365-2486.2010.02361.x)

411 Waller PJ, Ruby-Martin L, Ljungström BL, Rydzik A (2004) The epidemiology of abomasal  
 412 nematodes of sheep in Sweden, with particular reference to over-winter survival strategies.  
 413 Veterinary Parasitology, **122**, 207-220. (doi:10.1016/j.vetpar.2004.04.007)

414 Wang T, van Wyk JA, Morrison A, Morgan ER (2014) Moisture requirements for the  
 415 migration of *Haemonchus contortus* third stage larvae out of faeces. Veterinary Parasitology,  
 416 **204**, 258-264. (doi:10.1016/j.vetpar.2014.05.014)

417 Warszawski L, Frieler K, Huber V, Pontiek F, Serdeczny O, Schewe J (2014) The  
 418 Intersectoral Model Intercomparison Project (ISI-MIP): Project framework. Proceedings of  
 419 the National Academy of Sciences of the United States of America, **111**, 3228-3232

420



**Fig. 1.** Temperature-dependent *H. contortus*  $Q_0$  parameters in the absence of moisture limitations and with sheep stocking density (H) equal to 1. Parameters are defined in Table 1.

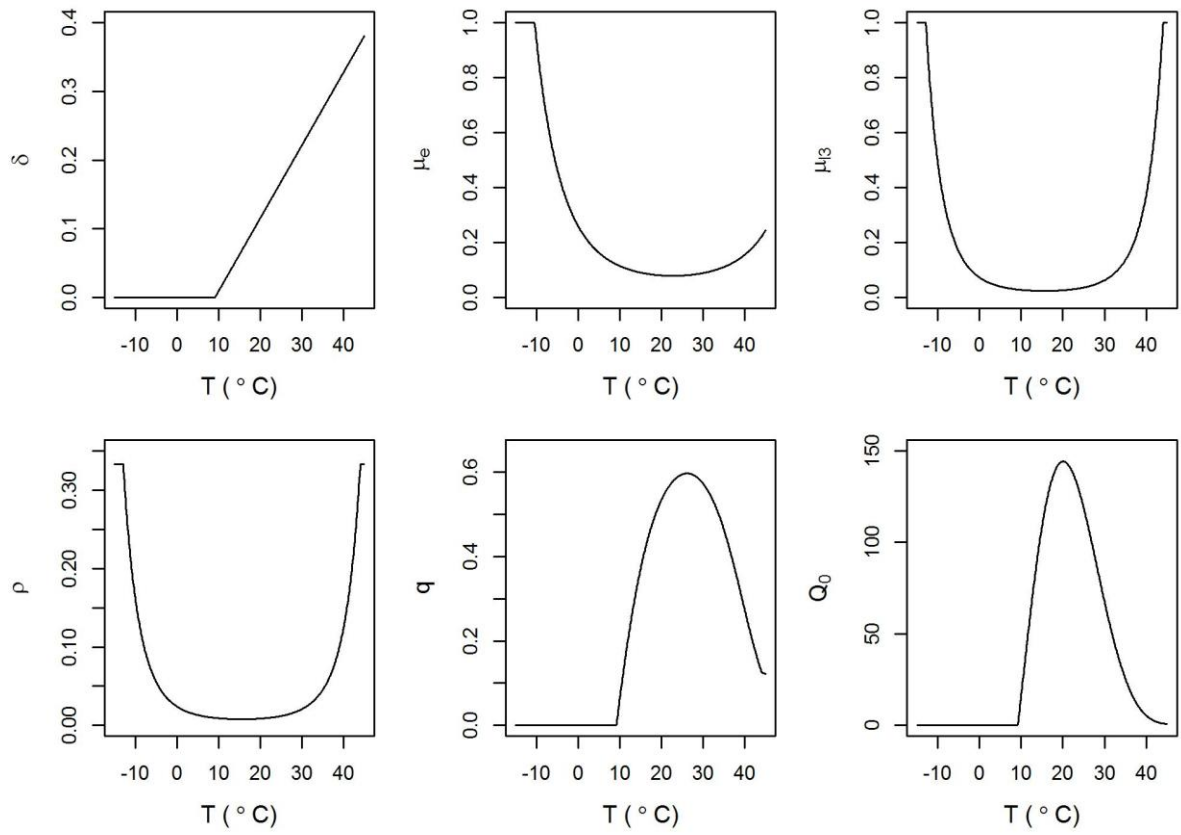
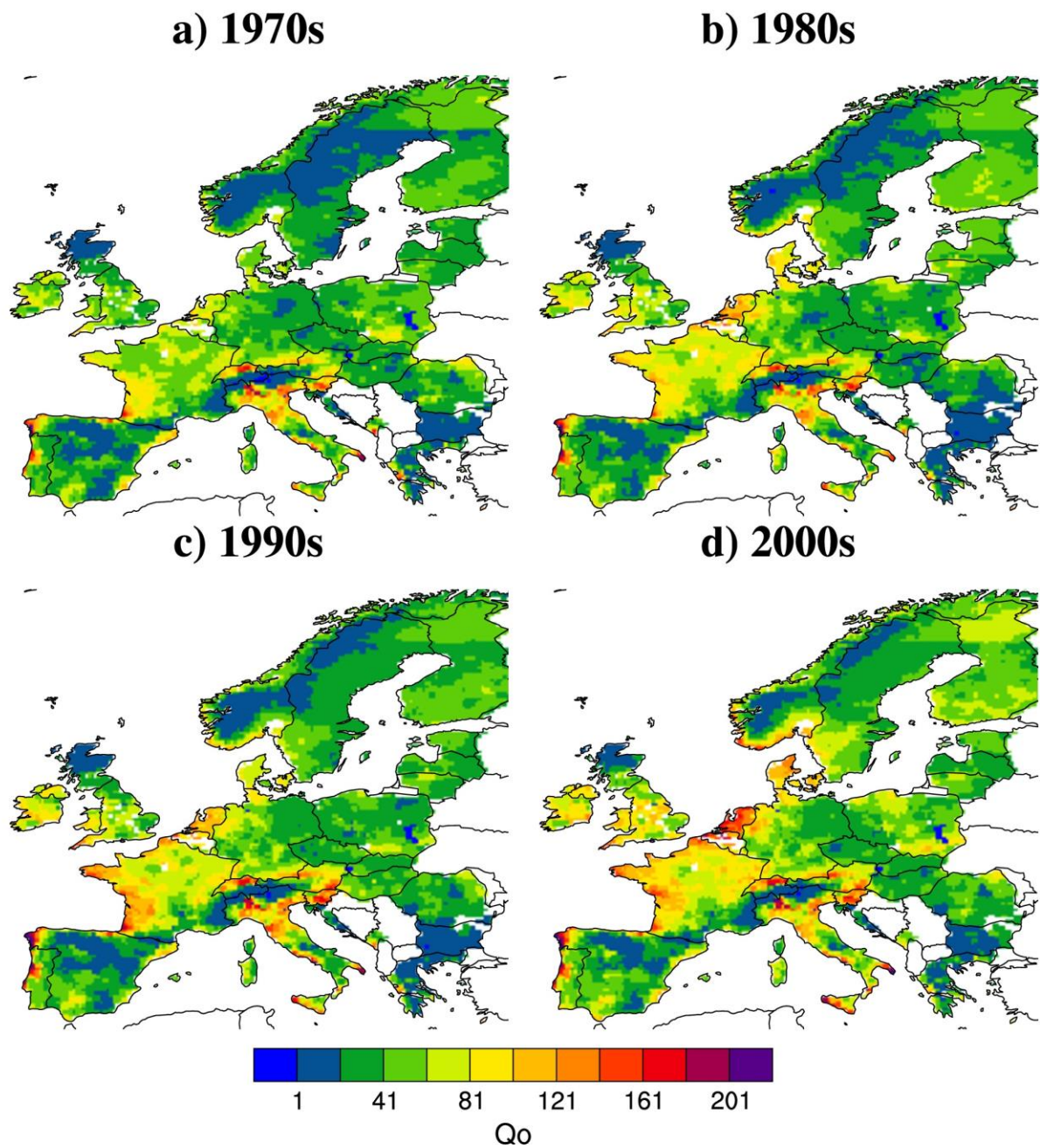


**Fig. 2.** Annual  $Q_0$  estimates for (a) the 1970s, (b) the 1980s, (c) the 1990s and (d) the 2000s using the EOBS climate dataset and regionally variable sheep stocking density (Fig. S1; Phelan *et al.*, 2014). The white shading depicts regions for which no sheep stocking density data were available.



428

429 **Fig. 3.** Annual  $Q_0$  estimates for (a) the 1970s, (b) the 1980s, (c) the 1990s and (d) the 2000s  
 430 using the EOBS climate dataset.  $Q_0\_HCT$  indicates that these simulations used a constant  
 431 sheep stocking density ( $H=1$ ). Note the difference in scale of  $Q_0$  compared with Fig. 2.

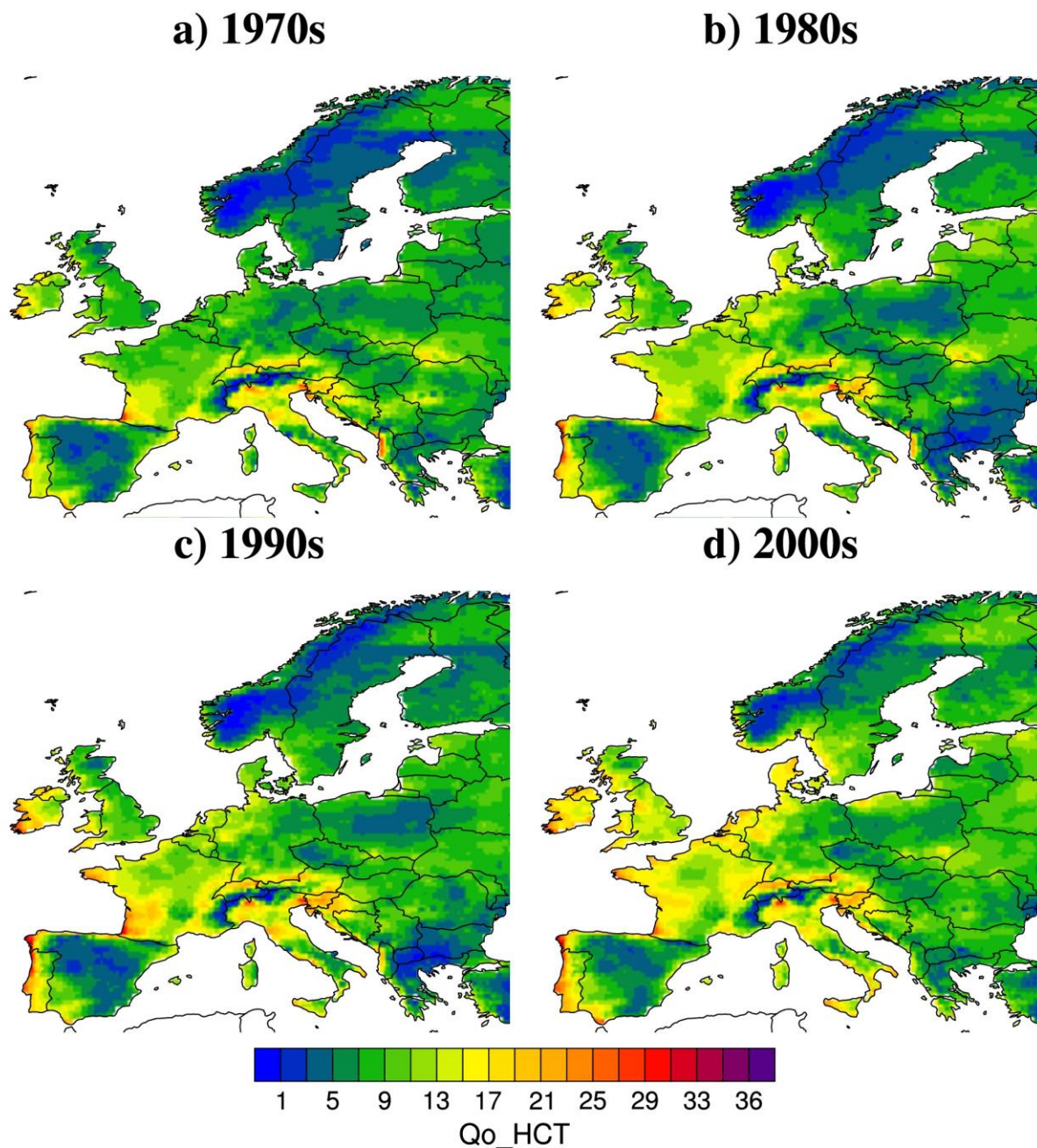


**Fig. 4.** Monthly  $Q_0$  estimates based on the EOBS climate data for 1970-2013 and a spatially variable sheep stocking density (Fig. S1; Phelan et al., 2015). The white shading depicts regions for which no sheep stocking density data were available.



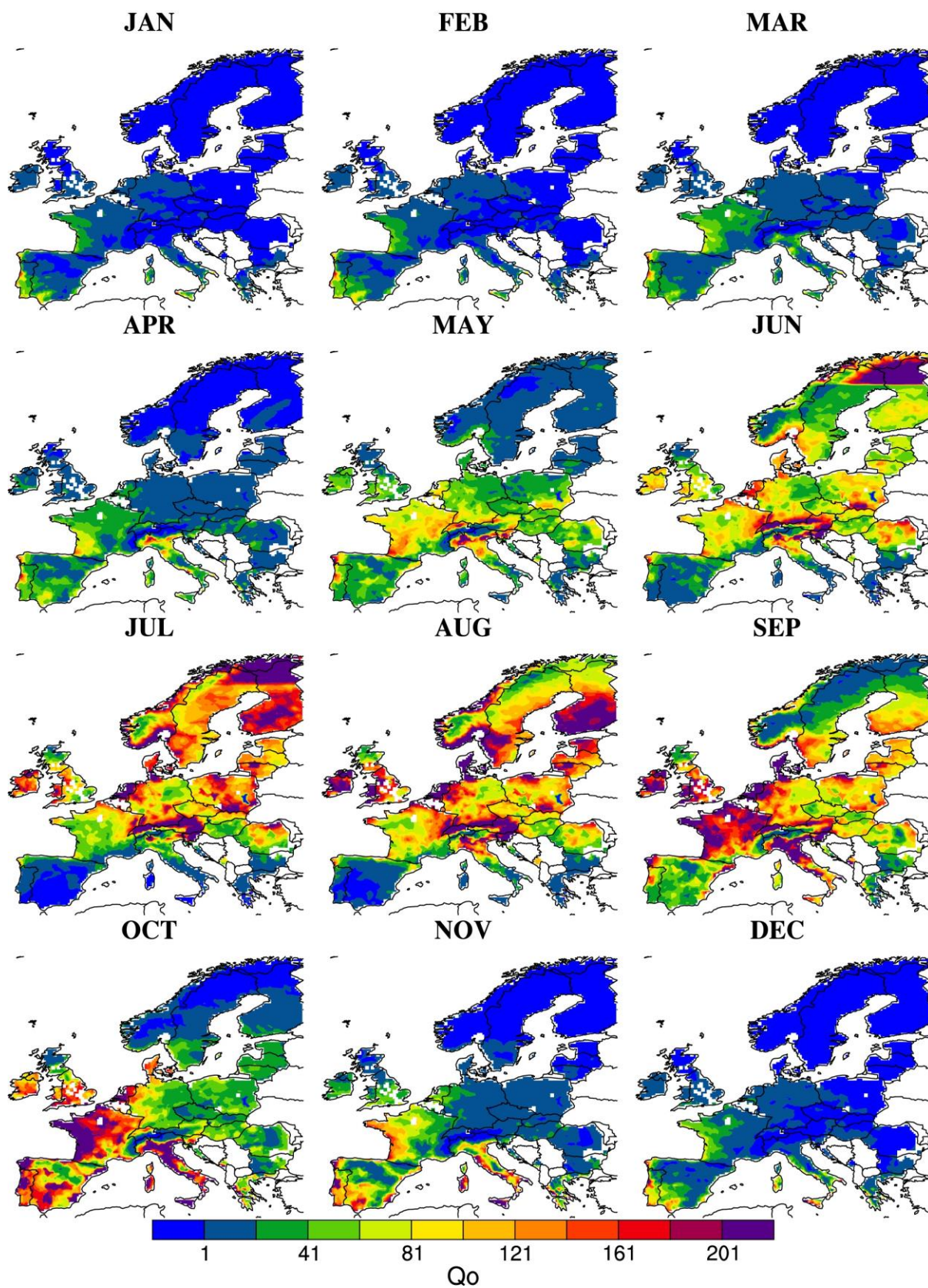


**Fig. 5.** Change in  $Q_0$  seasonality for (a) Northern Europe [48°N-59°N, 12°W-18.5°E] and (b) Southern Europe [35.5°N-44°N, 10°W-18.5°E]. The solid black line shows the  $Q_0$  model driven by the EOBS climate observations (1971-2010 average). The solid blue lines show the  $Q_0$  model driven by the ensemble mean over the same time period. The solid orange and red lines respectively show the ensemble mean of the  $Q_0$  simulations driven by the climate model ensemble for 2071-2090 under the RCP2.6 and RCP8.5 emission scenarios. Dotted lines depict the minimum and maximum within the model ensemble to assess the relative uncertainties.

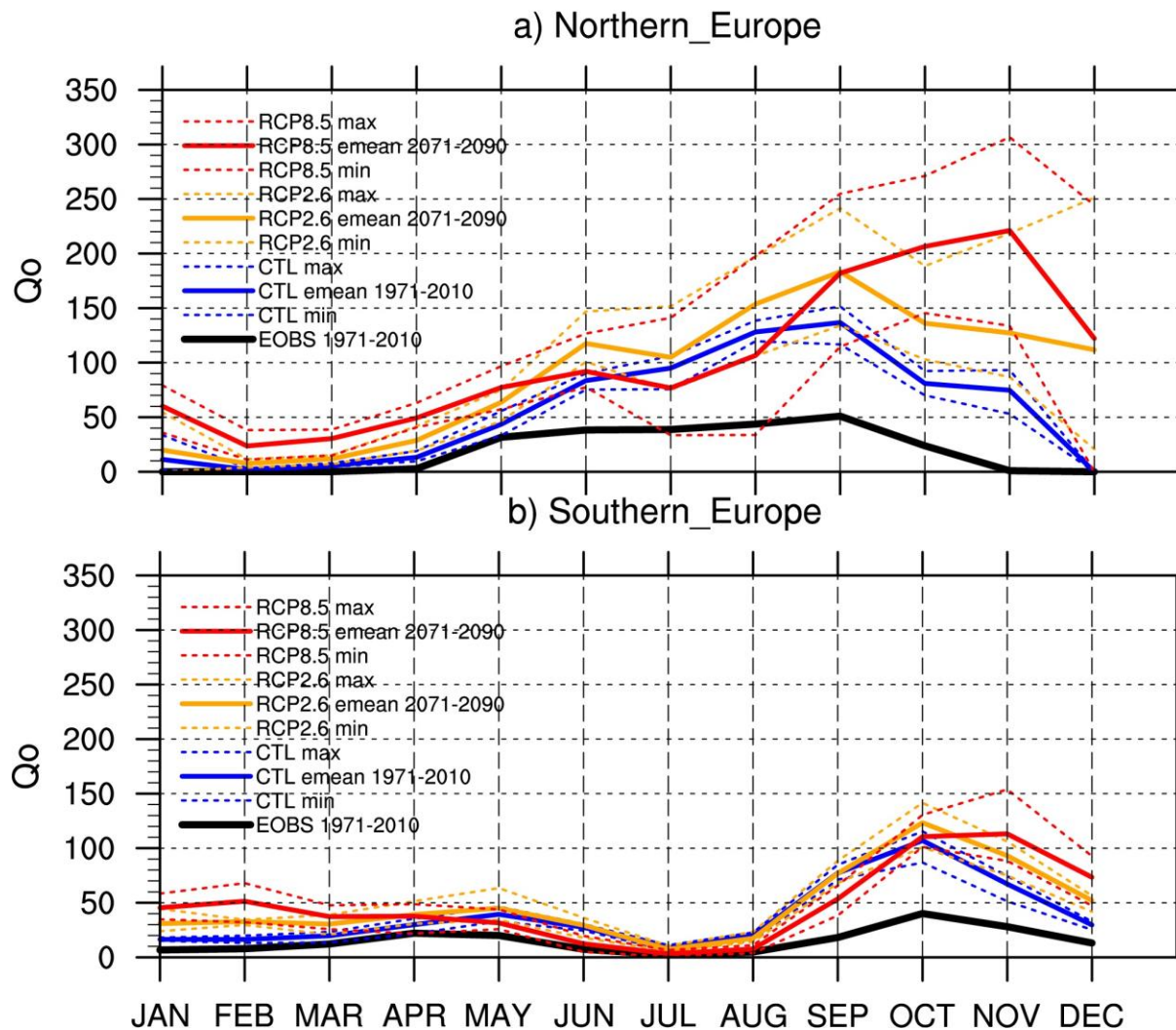




**Fig. 6.** Change in annual mean  $Q_0$  based on the ensemble mean (Emean) of five climate models shown as future predicted  $Q_0$  anomalies.  $Q_0$  was estimated using the five global climate models for different time slices (rows) and different emission scenarios (columns, lowest e.g. RCP2.6 to highest RCP8.5 emission scenario from left to right). Anomalies have been calculated with respect to the historical experiments (1951-2005 baseline). The white shading depicts regions for which no sheep stocking density data were available.

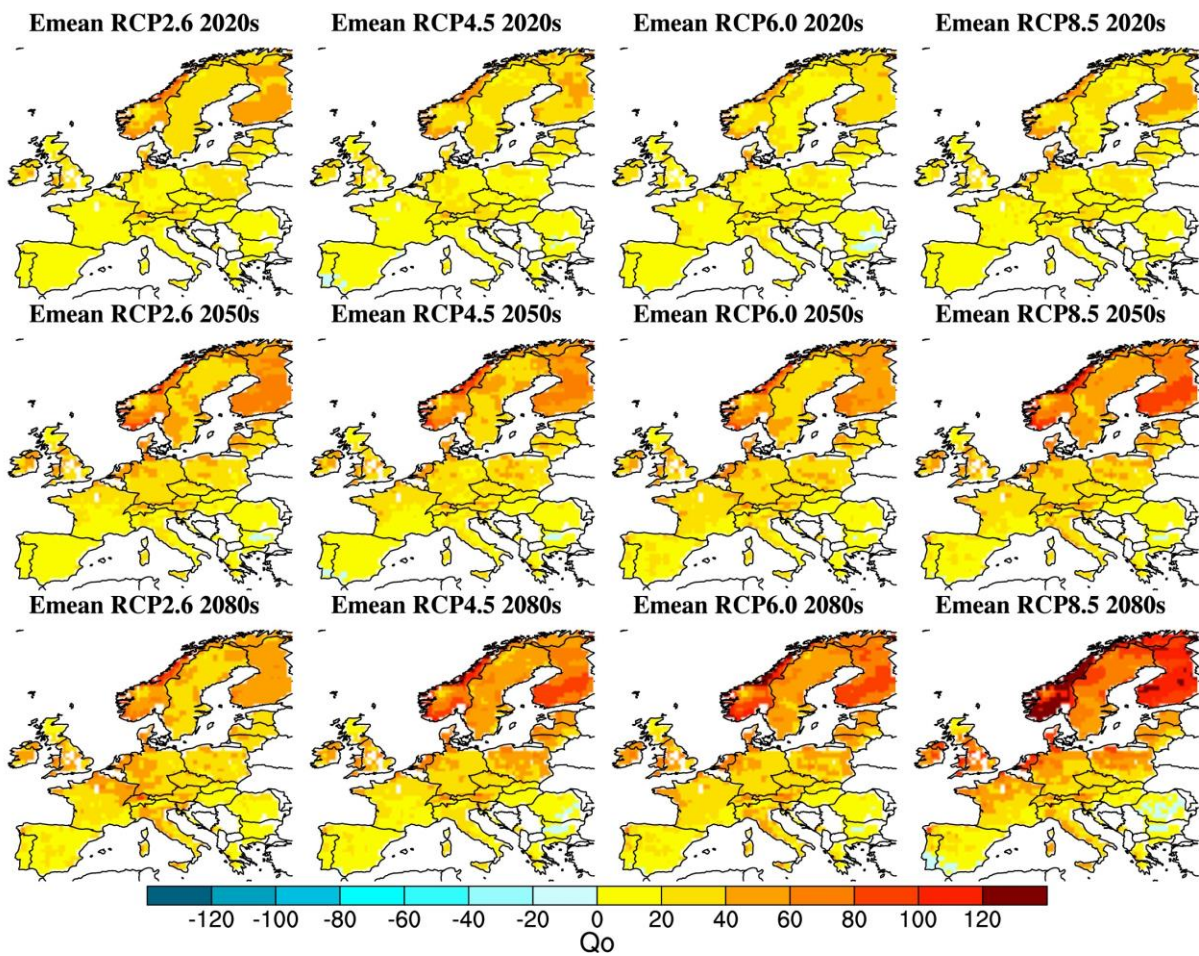
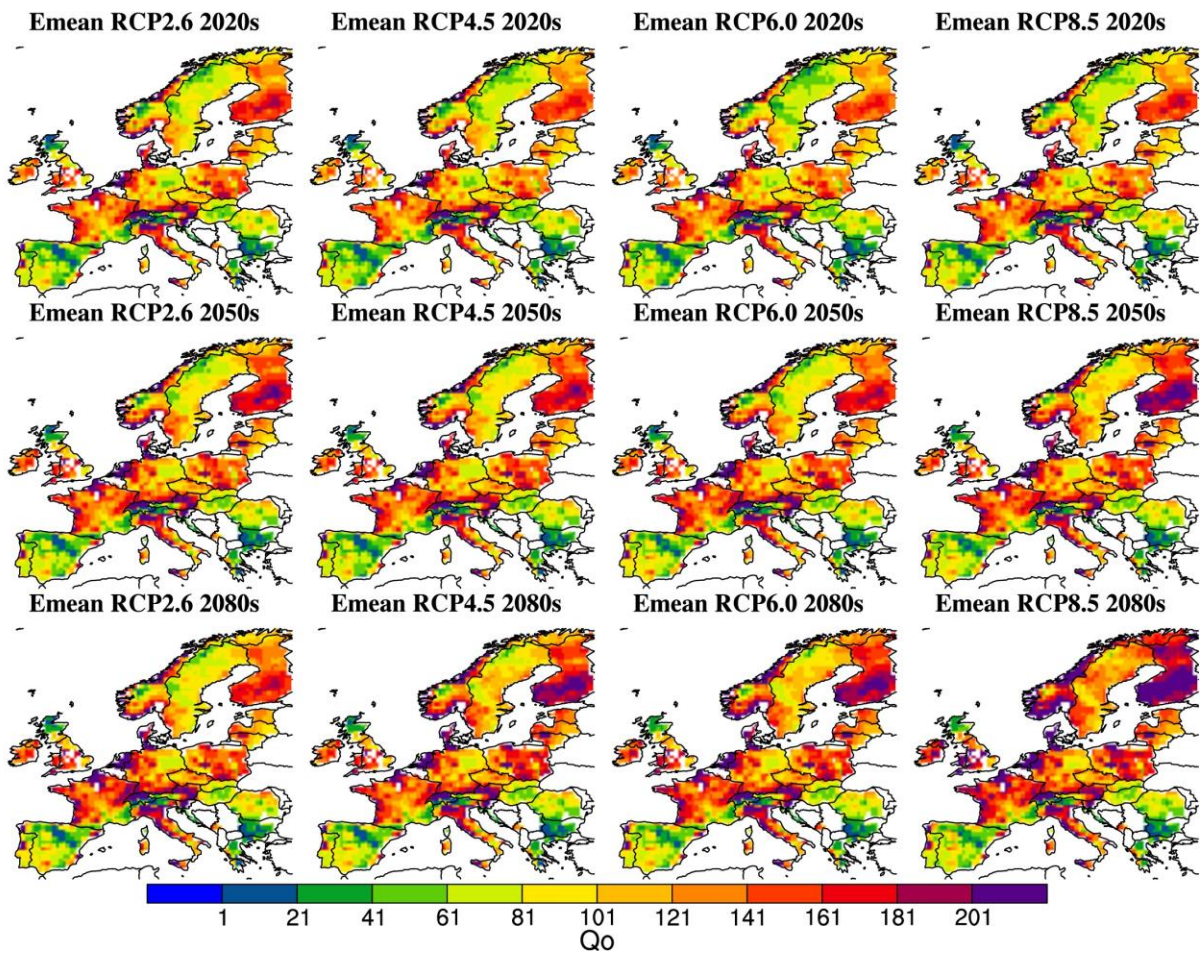


**Fig. 7.** Absolute annual mean  $Q_0$  values based on the ensemble mean (Emean) of five climate models.  $Q_0$  was estimated using the five global climate models for different time slices (rows) and different emission scenarios (columns, lowest e.g. RCP2.6 to highest RCP8.5 emission scenario from left to right). The white shading depicts regions for which no sheep stocking density data were available.



458

459





461 **Table 1.** Extended Q<sub>0</sub> model parameter definitions and estimates.

<i>Parameter</i>	<i>Definition</i>	<i>Value</i>	<i>Source</i>
<i>H. contortus</i>			
$\lambda$	Fecundity (eggs day <sup>-1</sup> adult <sup>-1</sup> )	2250	Coyne & Smith, 1992b
$\mu$	Instantaneous daily mortality rate of adult nematodes	0.05	Barger & LeJambre, 1988
$q$	Probability that an egg will develop to L3 and migrate onto pasture	$\begin{cases} \frac{\delta m_1}{(\mu_e + \delta)(\mu_{l3} + m_1)}, & P/E \geq 1 \\ 0, & P/E < 1 \end{cases}$	O'Connor et al., 2008; Khadijah et al., 2013; Rose et al., 2015b
$\delta$	Instantaneous daily development rate of eggs to L3	$-0.09746 + 0.01063T_{mean}$	Rose et al., 2015b

$\mu_e$	Instantaneous daily mortality rate of eggs	$\exp(-1.3484 - 0.10488T + 0.00230T_{mean}^2)$	Rose et al., 2015b
$\mu_{l3}$	Instantaneous daily mortality rate of L3 in faeces	$\exp(-2.62088 - 0.14399T + 0.00462T_{mean}^2)$	Rose et al., 2015b
$m_1$	Instantaneous daily L3 migration rate between faeces and pasture	0.25	Rose et al., 2015b
$\rho$	Instantaneous daily mortality rate of L3 on pasture	$\mu_{l3}/3$	Bolajoko et al., 2015
$m_2$	Proportion of total pasture L3 that are found on herbage	0.2	Callinan & Westcott, 1986; van Dijk & Morgan, 2011
$p$	Probability of establishment of ingested L3	0.4	Barger et al., 1985

---

**Host management**

$\beta$	Rate of ingestion of L3 on pasture	$\frac{c}{BA}$	-
$c$	Daily herbage dry matter intake per host (kg DM day <sup>-1</sup> )	1.4	Kao et al., 2000
$H$	Host density or stocking density (sheep ha <sup>-1</sup> )	Either regionally variable or held constant	Phelan et al., 2014
$B$	Standing biomass (kg DM ha <sup>-1</sup> )	2000	Leathwick et al., 1992; Kao et al., 2000
$A$	Grazing area (ha)	1	-

---

**Climate**

$P$	Total daily precipitation (mm)	Daily variable	Haylock et al., 2008; Taylor et al., 2012
$E$	Daily potential evapotranspiration (mm day <sup>-1</sup> )	$0.0023 \times 0.408 \times Ra \left( \frac{T_{max} + T_{min}}{2} + 17.8 \right) \sqrt{T_{max} - T_{min}}$	Hargreaves & Samani, 1985
$Ra$	Extra-terrestrial radiation (MJm <sup>-2</sup> day <sup>-1</sup> )	Daily variable	Anon, 2002
$T_{mean}$	Mean daily temperature (°C)	Daily variable	Haylock et al., 2008; Taylor et al., 2012
$T_{min}$	Minimum daily temperature (°C)	Daily variable	Haylock et al., 2008; Taylor et al., 2012
$T_{max}$	Maximum daily temperature (°C)	Daily variable	Haylock et al., 2008; Taylor et al., 2012

## SUPPORTING INFORMATION

Fig. S1. Livestock units (LSU) per hectare derived from Phelan et al. [32]. 1 LSU = 10 sheep.

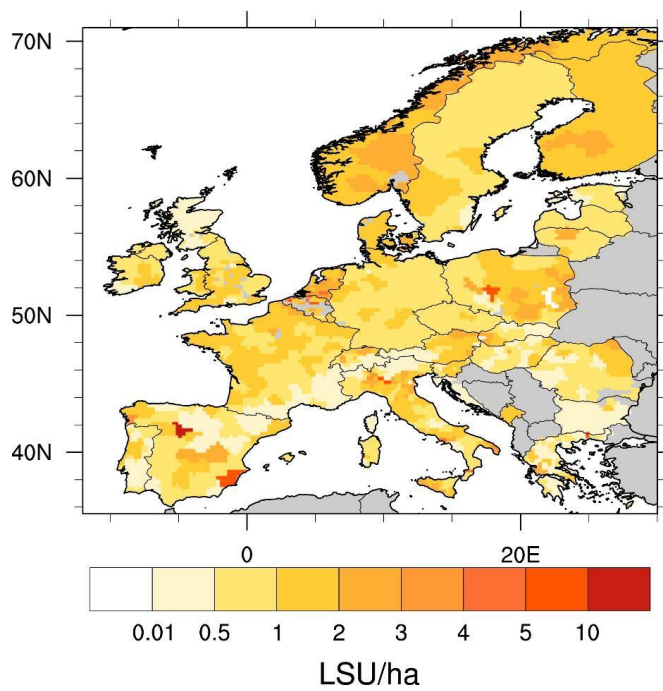


Fig. S2. Monthly  $Q_0$  estimates based on the EOBS climate data for the 1970s (1970-1979) and a spatially variable sheep stocking density (Fig. S1; *Phelan et al.*, 2014). The white shading depicts regions for which no sheep stocking density data were available.

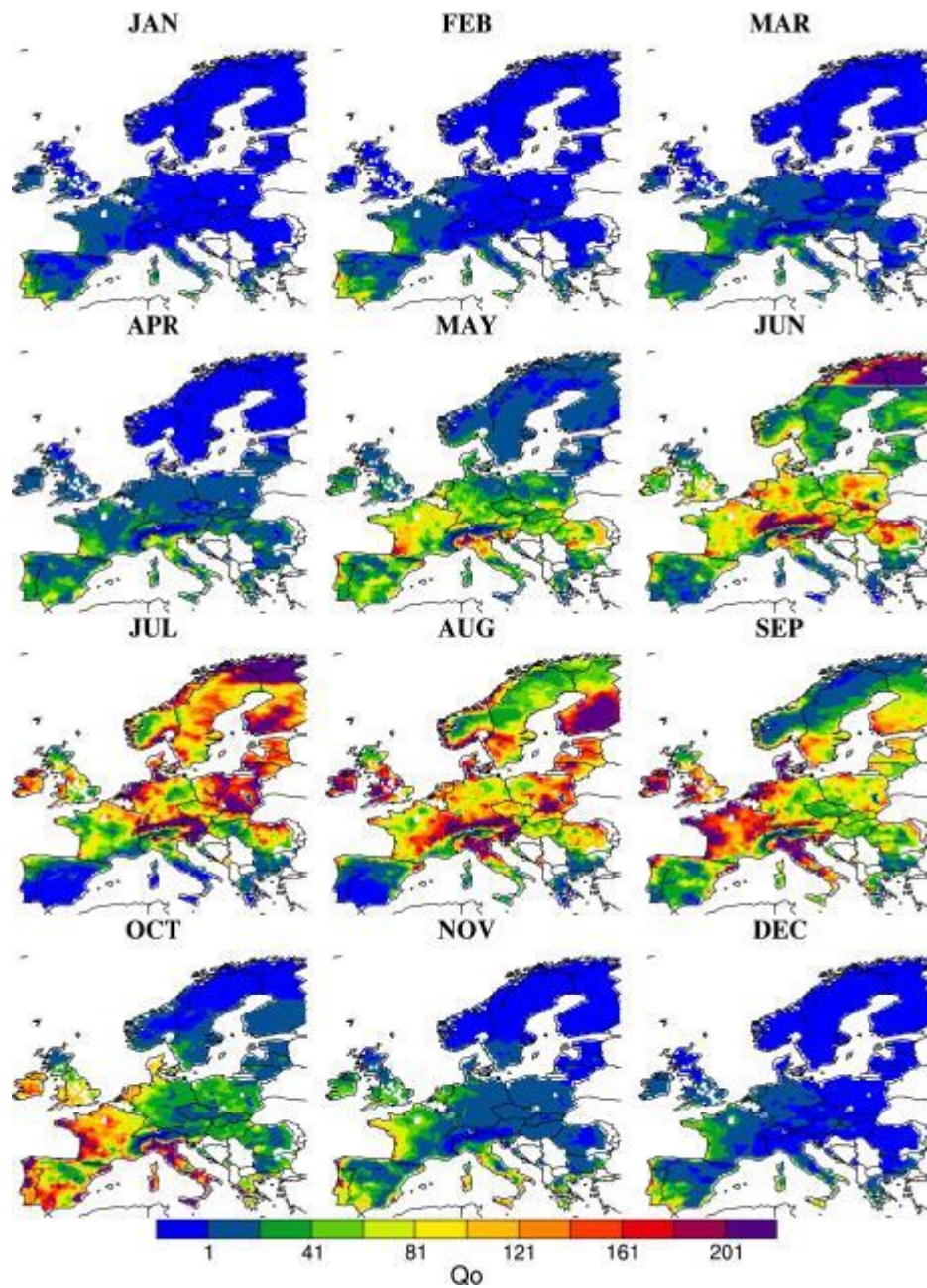




Fig. S2. Monthly  $Q_0$  estimates based on the EOBS climate data for the 1980s (1980-1989) and a spatially variable sheep stocking density (Fig. S1; Phelan *et al.*, 2014). The white shading depicts regions for which no stocking density data were available.

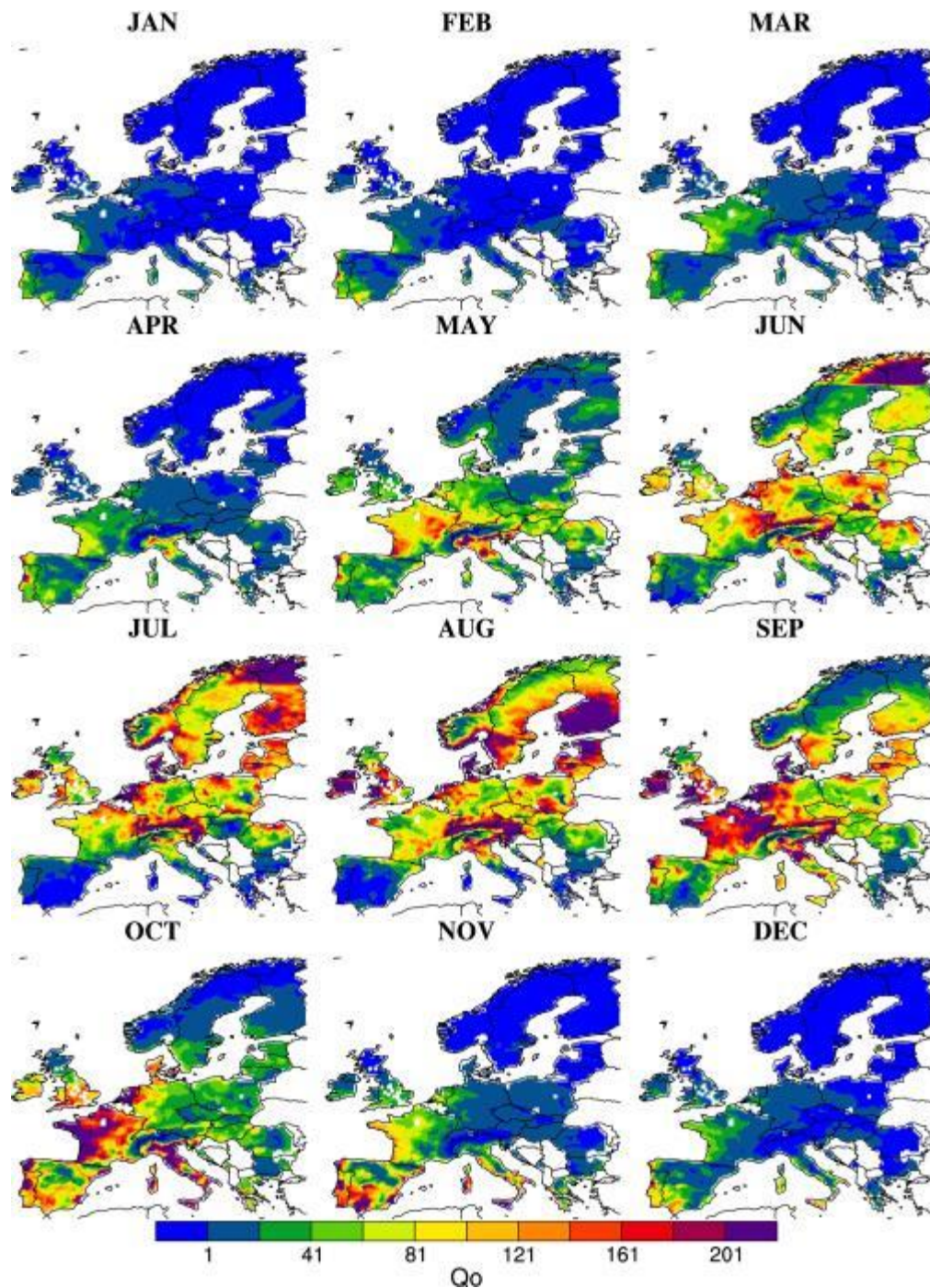


Fig. S3. Monthly  $Q_0$  estimates based on the EOBS climate data for the 1990s (1990-1999) and a spatially variable sheep stocking density (Fig. S1; Phelan *et al.*, 2014). The white shading depicts regions for which no stocking density data were available.

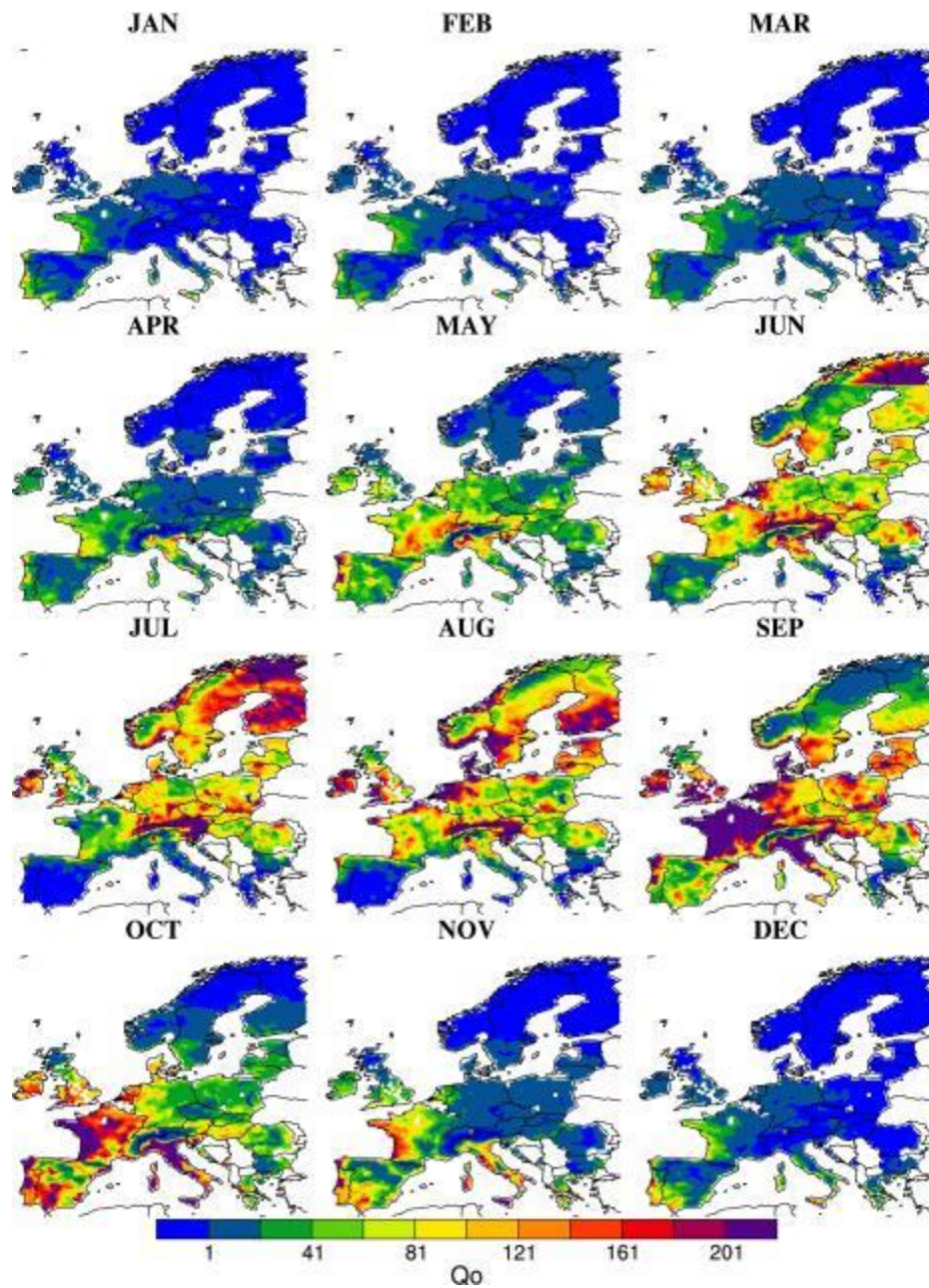




Fig. S4. Monthly  $Q_0$  estimates based on the EOBS climate data for the 2000s (2000-2009) and a spatially variable sheep stocking density (Fig. S1; Phelan *et al.*, 2014). The white shading depicts regions for which no stocking density data were available.

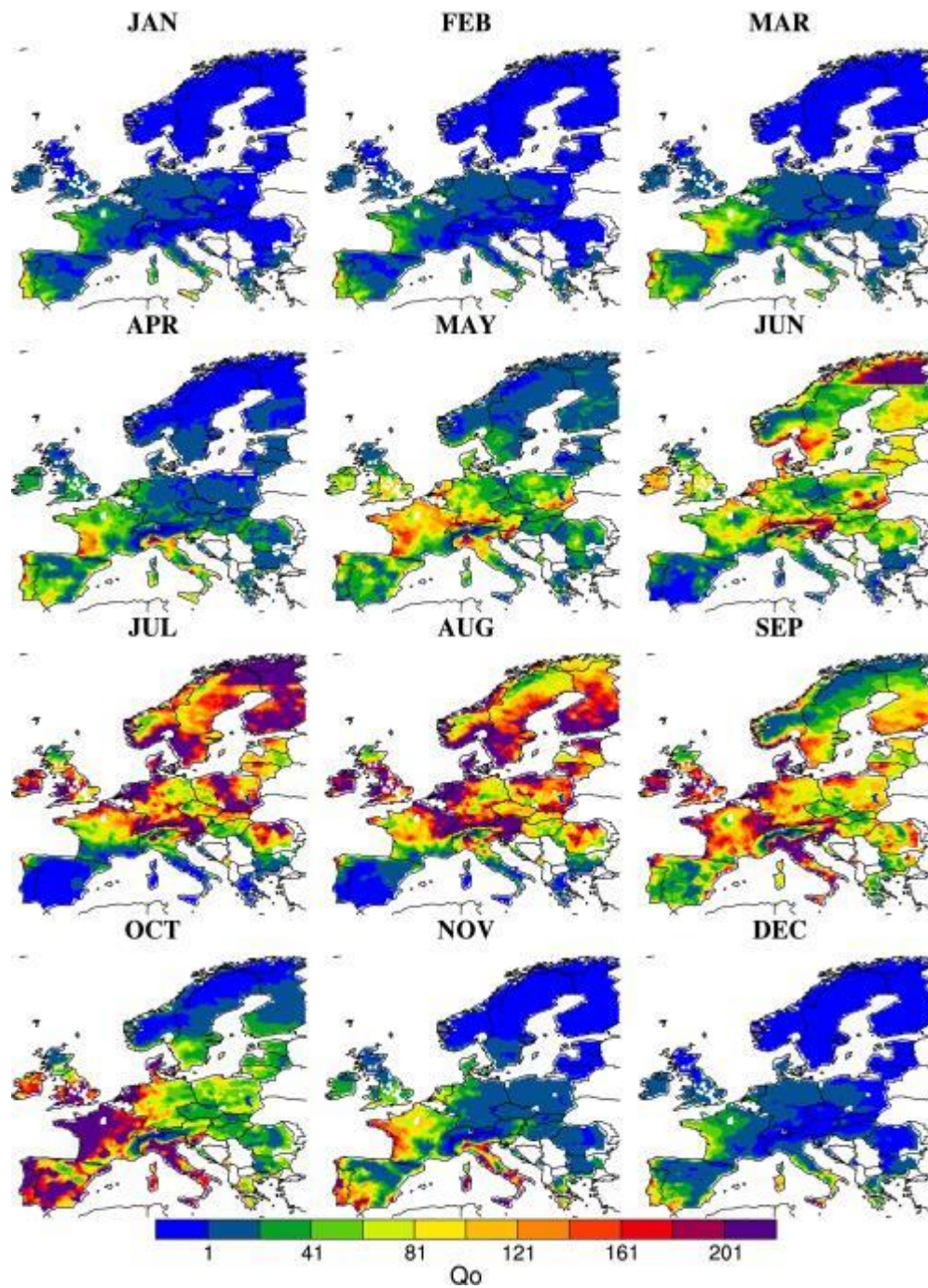


Fig. S5. Monthly estimates  $Q_0$  based on the EOBS climate data for 1970-2013 and a constant sheep stocking density ( $H=1$ ).

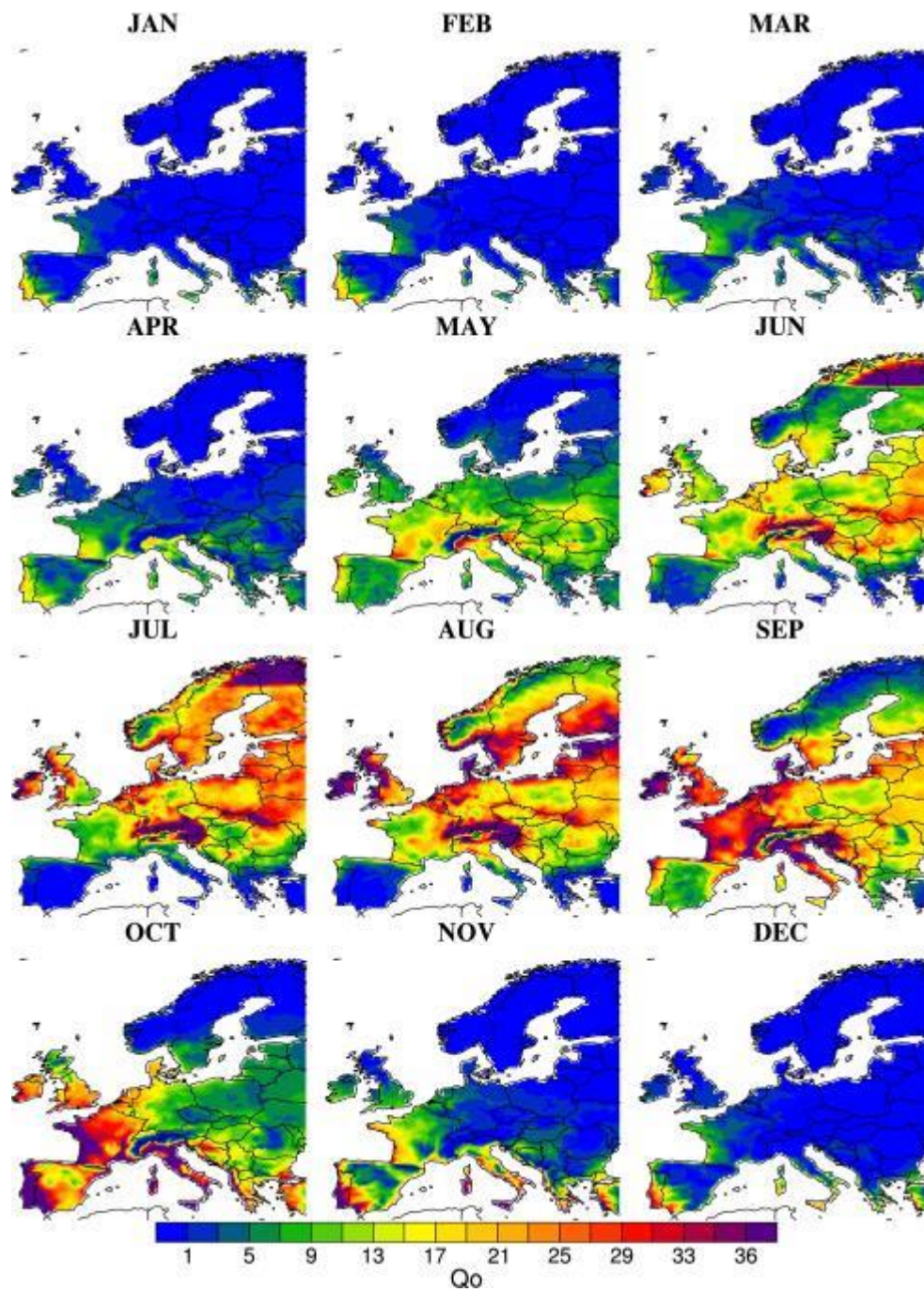




Fig. S6. Monthly  $Q_0$  estimates based on the EOBS climate data for the 1970s (1970-1979) and a constant sheep stocking density ( $H=1$ ).

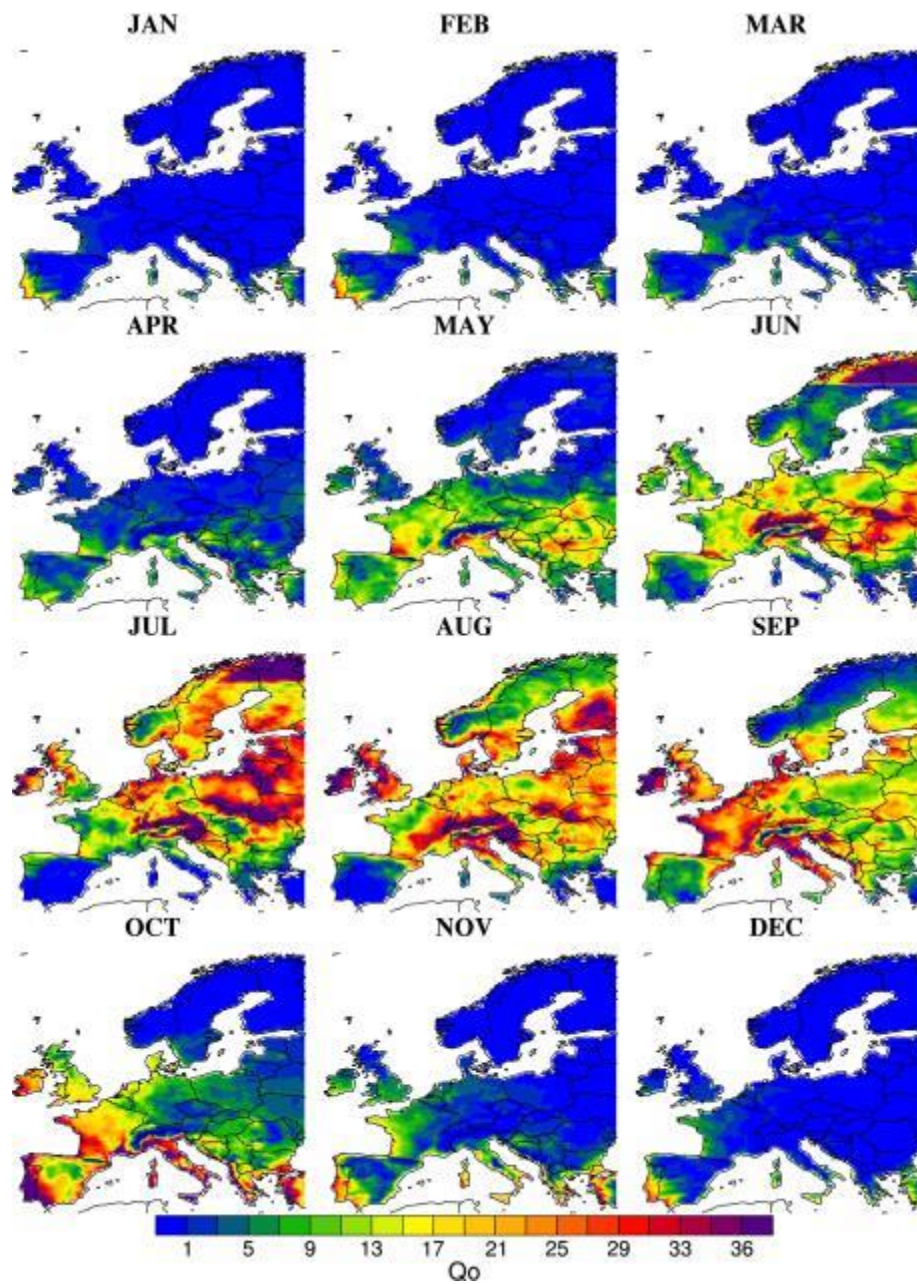


Fig. S7. Monthly  $Q_0$  estimates based on the EOBS climate data for the 1980s (1980-1989) and a constant sheep stocking density ( $H=1$ ).

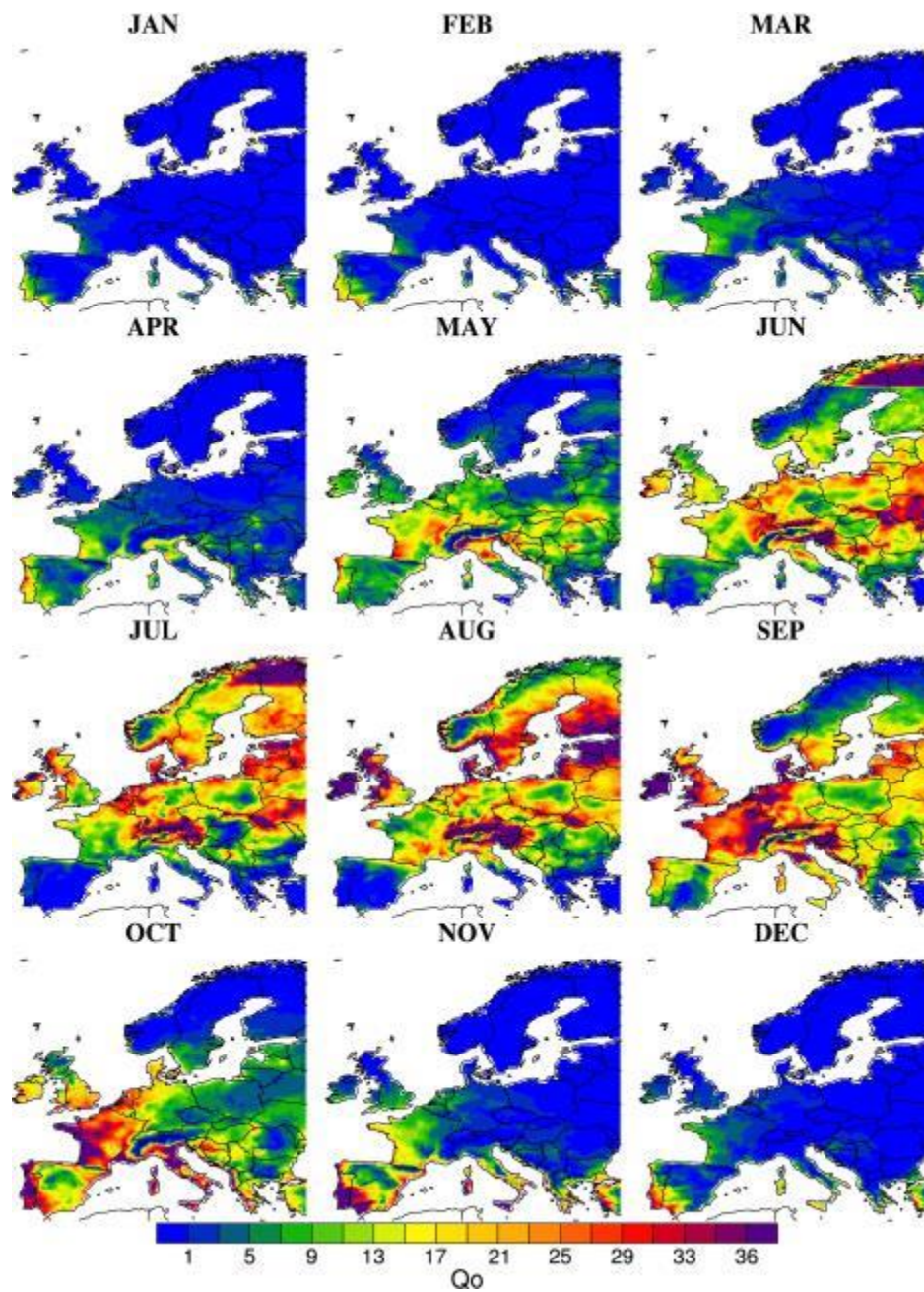




Fig. S8. Monthly  $Q_0$  estimates based on the EOBS climate data for the 1990s (1990-1999) and a constant sheep stocking density ( $H=1$ ).

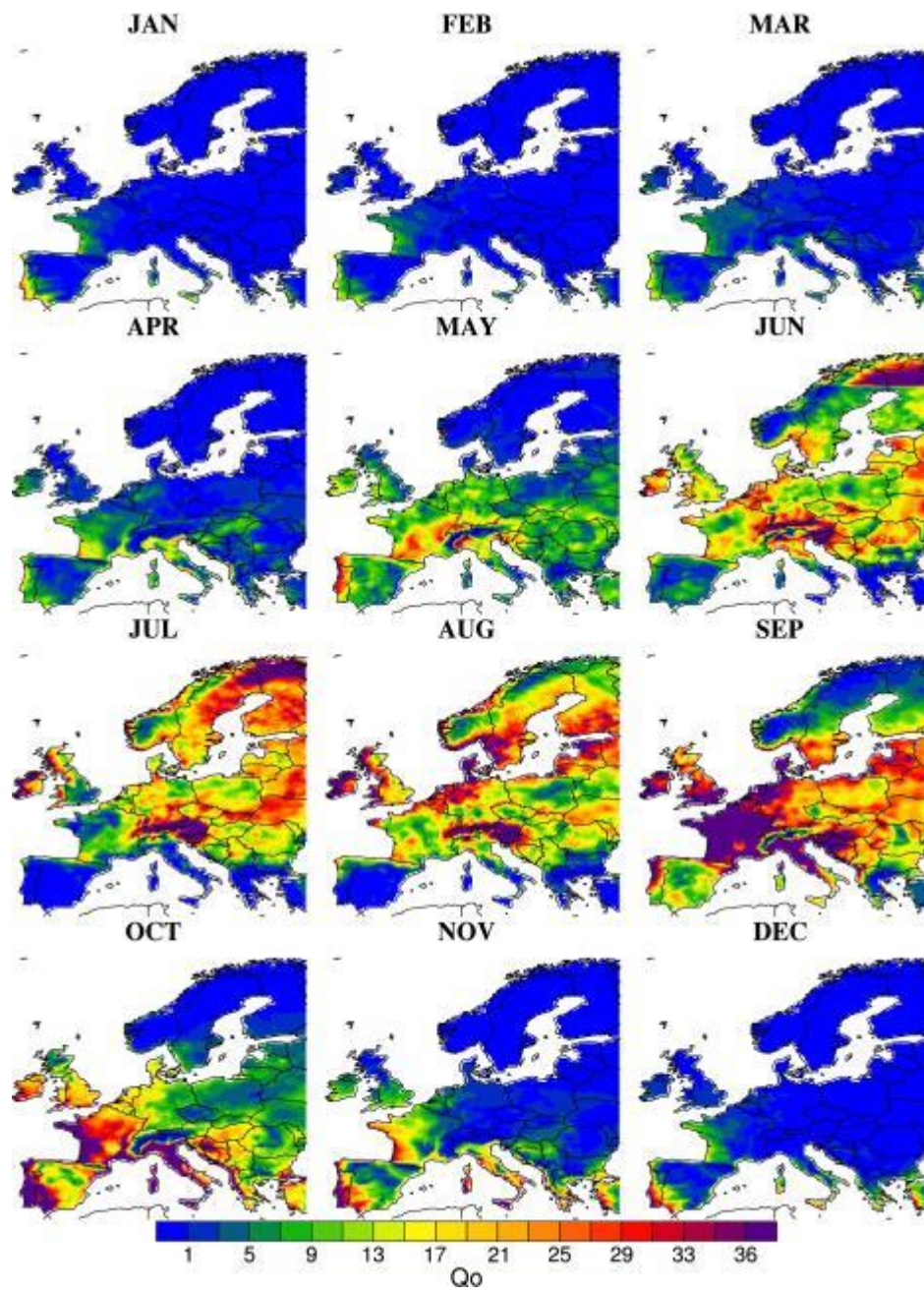


Fig. S9. Monthly  $Q_0$  estimates based on the EOBS climate data for the 2000s (2000-2009) and a constant sheep stocking density ( $H=1$ ).

